

Versatile Coordination Chemistry of Hexa-*tert*- Butyl-Octaphosphine

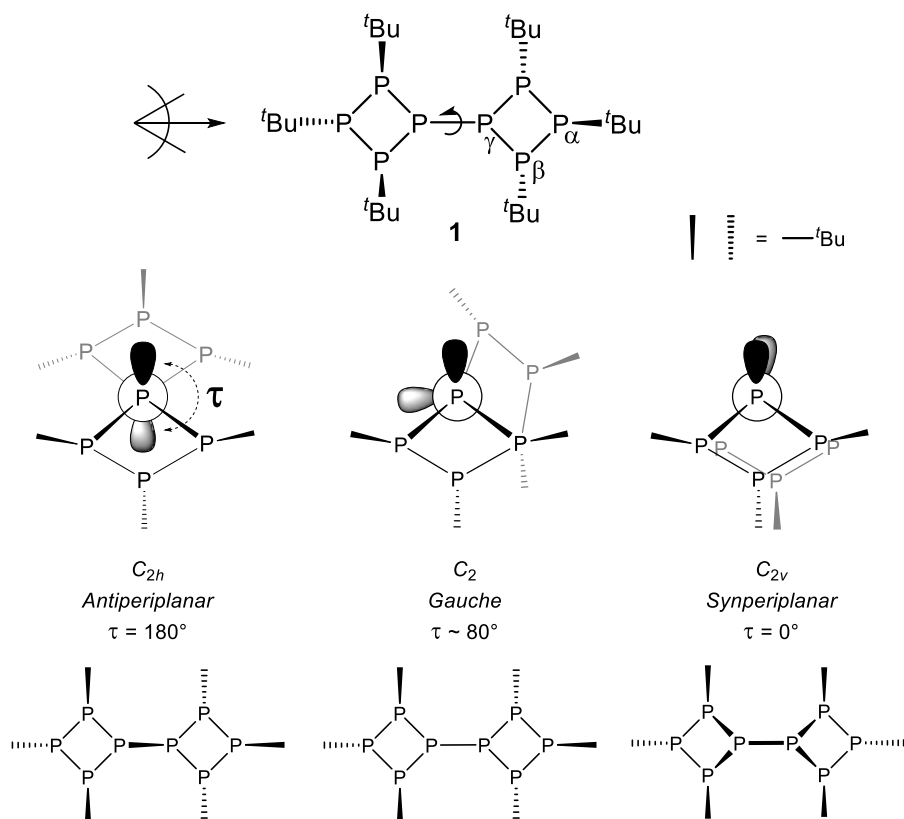
Toni Grell and Evamarie Hey-Hawkins*

Faculty of Chemistry and Mineralogy, Institute of Inorganic Chemistry, Johannisallee 29, 04103
Leipzig, Germany

ABSTRACT. The octaphosphine $\{\text{cyclo}-(\text{P}^t\text{Bu}_3)\}_2$ (**1**) possesses a multifaceted coordination chemistry. The predominant binding mode is a P,P-chelate, e.g. in the monometallic chelate complex $[\text{MLL}'(\mathbf{1}-\kappa^2\text{P}^2, \text{P}^{4'})]$ in which the ligand **1** adopts a *gauche* conformation. Examples include square-planar ($\text{M} = \text{Rh}^{\text{I}}$, $\text{L} = \text{CO}$, $\text{L}' = \text{Cl}$ (**2**), $\text{M} = \text{Pd}^{\text{II}}$, $\text{L} = \text{L}' = \text{Cl}$ (**3**), $\text{M} = \text{Pt}^{\text{II}}$, $\text{L} = \text{L}' = \text{Cl}$ (**9**)), tetrahedral ($\text{M} = \text{Co}^{-\text{I}}$, $\text{L} = \text{NO}$, $\text{L}' = \text{CO}$ (**4**)) and trigonal-planar complexes $[\text{ML}(\mathbf{1}-\kappa^2\text{P}^2, \text{P}^{4'})]$ ($\text{M} = \text{Pd}^0$, $\text{L} = \text{PPh}_3$, (**5**); $\text{M} = \text{Cu}^{\text{I}}$, $\text{L} = \text{Br}$ (**6**)). With two equivalents of $[\text{CuBr}(\text{SMe}_2)]$, a dinuclear complex $[(\text{CuBr})_2(\mathbf{1}-\kappa^2\text{P}^2, \text{P}^{2'}, \kappa^2\text{P}^4, \text{P}^{4'})]$ (**7**) was obtained which features a *synperiplanar* conformation of the octaphosphine. A second coordination mode was also observed in $[\text{PtCl}_2(\mathbf{1}-\kappa^2\text{P}^1, \text{P}^{2'})]$ (**10**) in which the bridge phosphorus atom in octaphosphine **1** is involved in the chelation, with the ligand in an *antiperiplanar* conformation. Thermolysis of selected complexes showed them to be suitable candidates for the generation of phosphorus-rich metal phosphides MP_x ($x > 1$).

Introduction. Phosphorus-rich compounds are a fascinating class of substances as their similarity to organic compounds is a vivid example for the isolobal concept.¹ Ever since *cyclo*-P₅Ph₅,^{2,3} the archetype of this class of compounds, was discovered almost 150 years ago, a vast number of molecules^{4,5} were added to this library. Polyphosphorus compounds can thus exhibit constitutional, configurational as well as conformational isomerism and furthermore also multiple bonds⁶ and even aromaticity⁷ which is one of the reasons why phosphorus is referred to as the carbon copy⁸. Due to the lone pair of electrons and the high number of phosphorus atoms and thus potential binding modes, the coordination chemistry of these compounds is fascinating.⁴ For instance, the reaction of P₇Et₃ with [Cr(CO)₅(thf)] already yields five different mono-, di- and trinuclear complexes.⁹

Nevertheless, the coordination behavior of phosphorus-rich compounds was only sparsely investigated. This is due to their usually challenging synthesis owing to rather unselective formation reactions as well as a pronounced tendency to undergo transformation reactions to other phosphines. Therefore, we have developed rational syntheses for phosphorus-rich ligands and investigated their coordination chemistry over the last years. Selective syntheses for *cyclo*-(P₅^tBu₄)⁻ and (P₄R₄)²⁻ (R = ^tBu, Ph, 2,4,6-Me₃C₆H₂)¹⁰ allowed the preparation of numerous novel metal complexes¹¹⁻¹³ as well as the discovery of several unexpected reactions thereof^{14,15}. We were furthermore able to show that these compounds can be converted to phosphorus-rich metal phosphides MP_x (x > 1) by mild thermolysis^{16,17} provided the right organic substituents are used¹⁸. This provides, therefore, a simple way to obtain these interesting materials, which are usually very hard to obtain.¹⁹



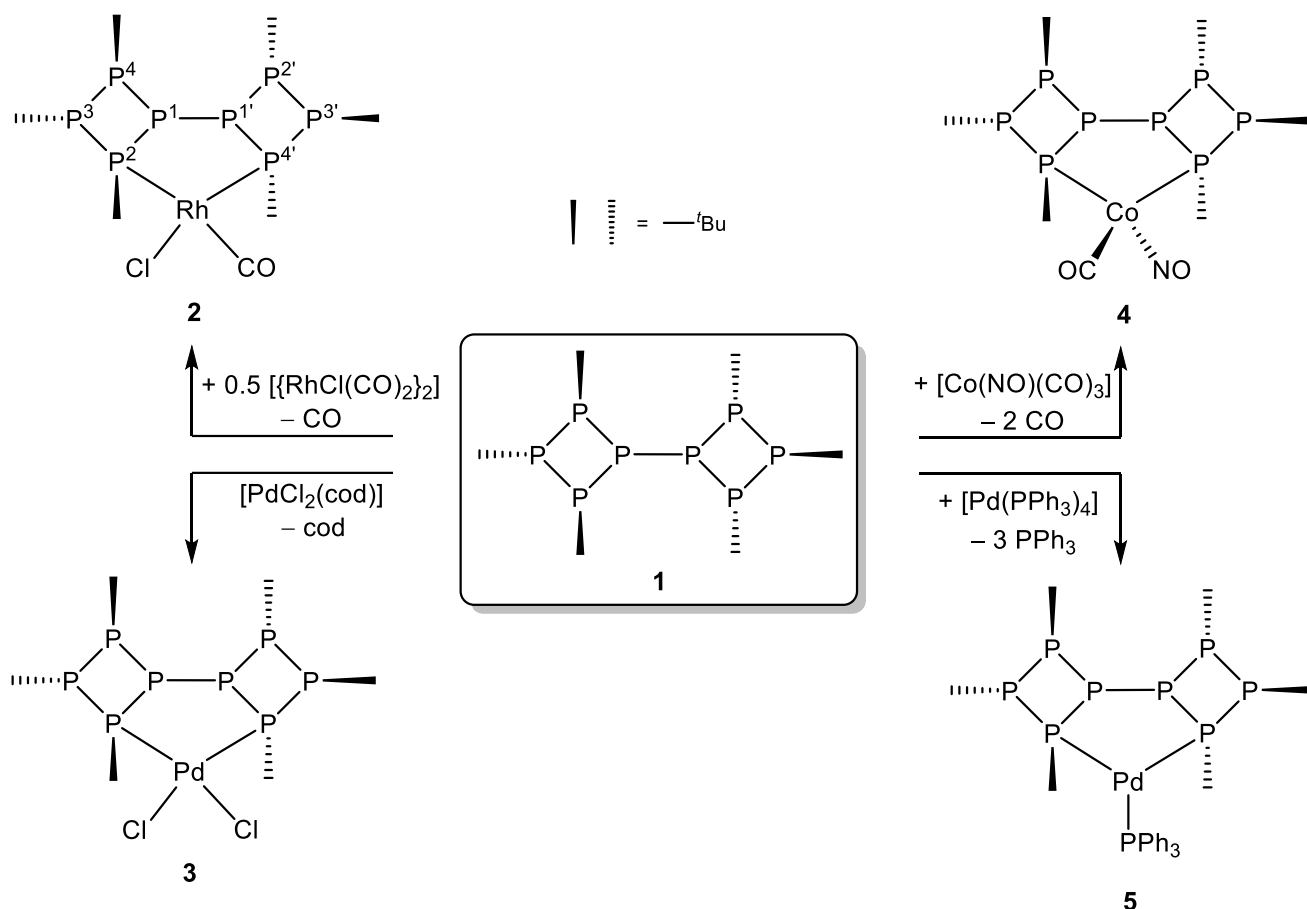
Scheme 1. Structural formulas and Fischer projections of the rotamers of octaphosphine **1**.

Very recently, we reported the facile synthesis of octaphosphine $\{cyclo-(P_4^tBu_3)\}_2$ (**1**) and formation of mono-, di- and trinuclear gold(I) chloride complexes.²⁰ Accordingly, there are two rotamers of octaphosphine **1** (Scheme 1) with *antiperiplanar* and *gauche* conformation which are practically isoenergetic and represent energetic minima, as well as a third one with *synperiplanar* conformation representing a maximum only slightly higher in energy ($\Delta E_{rel} = +29.6 \text{ kJ}\cdot\text{mol}^{-1}$). They are defined by the dihedral angle (τ) between the bridge P atoms (designated γ -P) and their lone pairs of electrons. The phosphine can freely rotate around this P–P bond as the barriers between the rotamers are very low ($\Delta E_{act} = +10.9 \text{ kJ}\cdot\text{mol}^{-1}$) which leads to a highly dynamic behavior in the respective mono-, di- and trinuclear gold(I) complexes in solution.²⁰

Furthermore, only the phosphorus atoms adjacent to the bridge atoms (designated β -P, Scheme 1) are involved in coordination to gold(I).

Attempts to extend the coordination chemistry of octaphosphine **1** to other metal complexes suggested that the coordination properties of **1** are rather limited, as in many cases instead of complexation the octaphosphine surprisingly rearranged to its constitutional isomer 2,2',2'',2''',3,3'-hexa-*tert*-butyl-bicyclo[3.3.0]octaphosphane with pentalane structure.²¹ However, with the right choice of metal precursor complexes, the versatile coordination behavior of this phosphorus-rich molecule can be elucidated, as shown here.

Results and Discussion. Octaphosphine **1** readily reacts with the rhodium precursor complex $[\{\text{RhCl}(\text{CO})_2\}_2]$ with loss of CO to give $[\text{RhCl}(\mathbf{1}-\kappa^2P^2, P^4)(\text{CO})]$ (**2**, Scheme 2). All analytical data confirm the formation of a mononuclear chelate complex with C_1 symmetry. No further coordination occurs by adding additional equivalents of the metal complex precursor.



Scheme 2. Reaction of octaphosphine **1** to give the mononuclear chelate complexes **2**, **3**, **4** and **5** with the numbering scheme shown for **2**.

Crystals of **2** were previously obtained as a side product from the reaction of $\text{Na}\{\text{cyclo}-(\text{P}_5^{\text{tBu}})_4\}$ with $[\{\text{RhCl}(\text{CO})_2\}_2]$, presumably due to octaphosphine **1** as impurity in the starting material.²² The molecular structure (Figure 1, structural parameters given in Table 1) shows that two of the β -P atoms in ligand **1** act as donor atoms and form a five-membered ring with the rhodium atom which is in a slightly distorted square-planar coordination environment (τ_4' for four-coordinate transition metals²³ is 0.08). Obviously, this requires a *gauche* conformation of the ligand ($\tau = 78.29(5)^\circ$). The coordination furthermore induces a significantly shorter bond length between the γ -P atoms of the phosphine (P(4)–P(5), $\Delta(\text{P}–\text{P}) \approx 0.07 \text{ \AA}$) as well as a tilting of the two four-membered P rings toward the metal atom. The Rh–P bond trans to the CO ligand is

considerably longer than the second one, due to the different *trans* effects of the co-ligands.²⁴ All remaining parameters such as P–P, Rh–Cl and Rh–C bond lengths are within normal range.

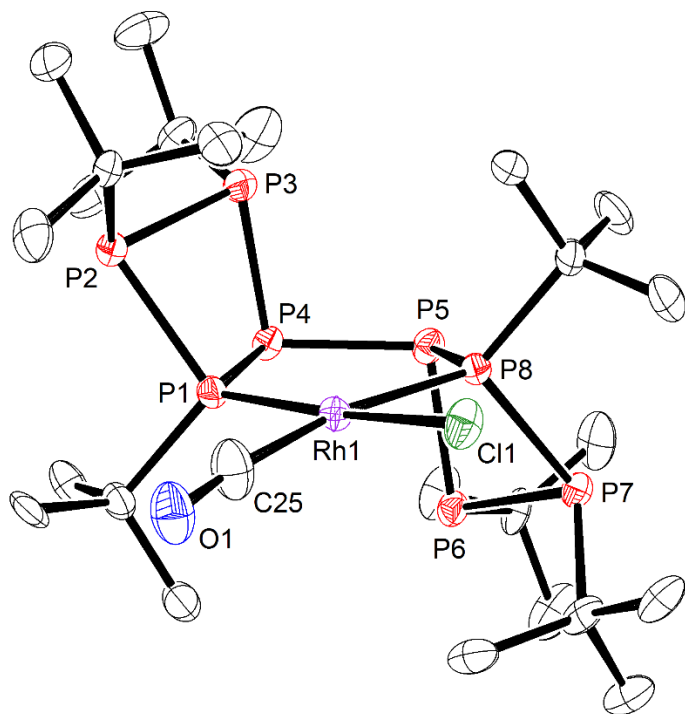


Figure 1. Molecular structure of complex **2**. Selected structural parameters are given in Table 1.

The $^{31}\text{P}\{^1\text{H}\}$ NMR spectrum of **2** is shown in Figure 2 (top). Even though the ligand in complex **2** possesses C_2 symmetry, the complex itself has C_1 symmetry due to the different co-ligands on the Rh atom. Accordingly, the phosphorus atoms are rendered chemically and magnetically nonequivalent, and thus eight multiplets can be discerned. Including the NMR active ^{103}Rh nucleus ($I = 1/2$, $\text{NA} = 100\%$), the spectrum of complex **2** thus corresponds to an ABCDEFGHX spin system which could be successfully simulated (Figure 2, bottom). Selected NMR parameters from the simulation are given in Table 1 (complete list in Experimental Section). The results of the simulation are in excellent agreement with a mononuclear chelate complex. Most importantly, the $^1J_{\text{PP}}$ coupling constants confirm the expected connectivity of the phosphorus

atoms within the ligand. They are negative and range between -149.0 Hz and -198.0 Hz, which matches well with t Bu substituted P atoms in four-membered P-rings of similar compounds.²⁵⁻²⁸ The sole exception to this is the coupling between the bridgehead P atoms ($^1J_{P(E)-P(H)} = -318.7$ Hz) which is usually smaller in similar compounds.^{29,30} However, XRD analysis shows that this increase corresponds well with the reduction of the respective bond length. This correlation has been described for other phosphorus-rich compounds³¹ and is similarly observed here for the $^1J_{P-Rh}$ coupling constants and the Rh-P bond lengths in complex **2**. The coupling between Rh and the donor atom P_B *trans* to CO is considerably larger than to the one in *cis* position (P_A) and has in turn a larger bond length. Additionally, this nucleus experiences a smaller deshielding. These observations agree well with similar rhodium(I) complexes^{32,33} and are caused by the *trans* effect of the CO ligand. The $^2J_{PP}$ coupling constants provide additional stereochemical information. For P-P couplings within all-*trans* substituted four-membered rings, they vary from $+22.4$ to $+44.9$ Hz which is in good agreement with similar compounds.²⁵⁻²⁸ The $^2J_{PP}$ coupling constants between P_E and P_G as well as P_F and P_H are exceptionally large and positive. This indicates a parallel orientation of the respective lone pairs of electrons³⁴ and therefore confirms the *gauche* conformation of the ligand as observed in the solid state. The coupling constants of the donor atoms P_A and P_B are rather small (4.4 Hz) suggesting a *cis* coordination of the metal atom.³⁵ The results from $^{31}P\{^1H\}$ NMR spectroscopy therefore confirm the constitution, configuration as well as the conformation of complex **2** in solution to be identical with the solid state.

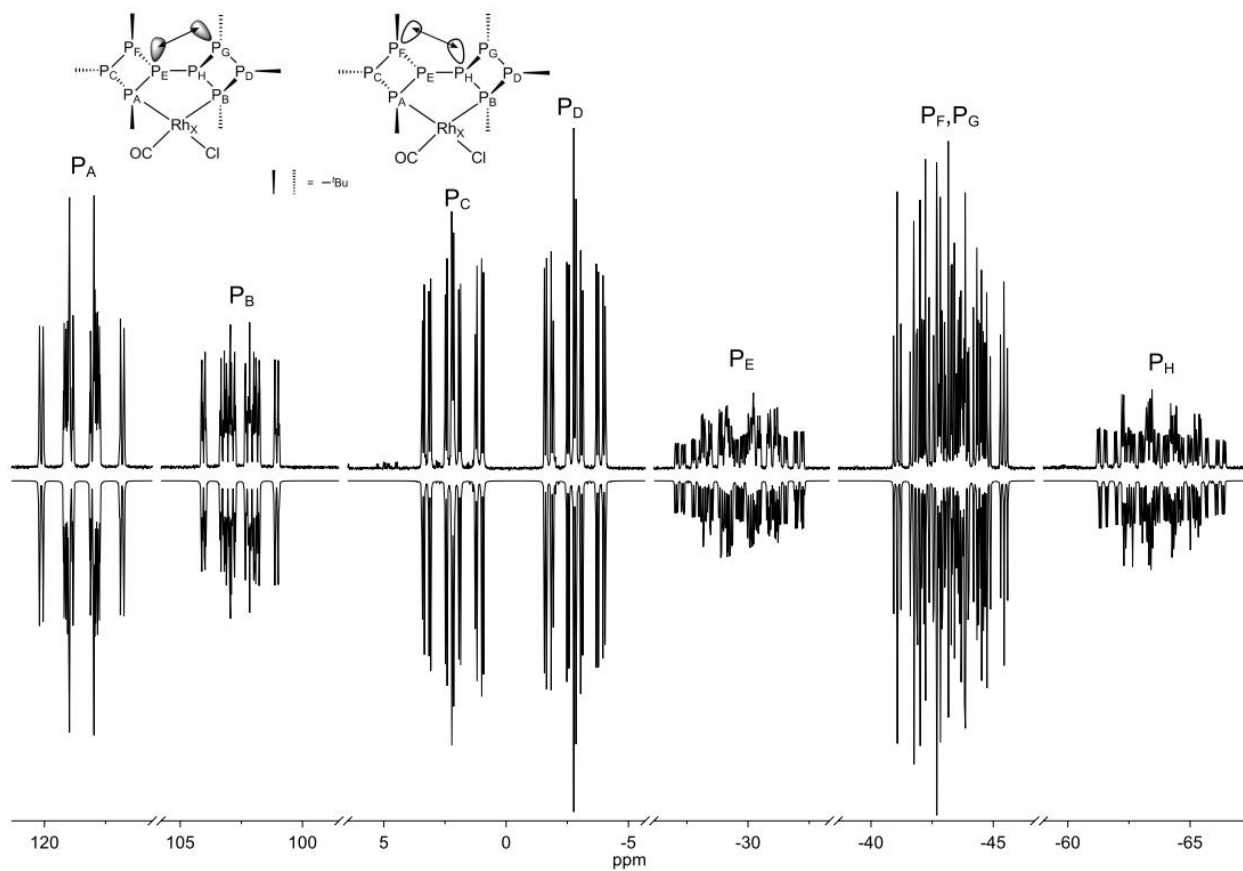


Figure 2. Experimental (top) and simulated (bottom) $^{31}\text{P}\{^1\text{H}\}$ NMR spectrum of complex **2** including schemes for the assignment and demonstration of the stereochemical origin of the $^2J_{\text{PP}}$ coupling constants.

Furthermore, elemental analysis as well as mass spectrometry confirm the composition of complex **2**. The mass spectrum shows peaks related to the ions $[\text{M}-\text{CO}-\text{Cl}]^+$, $[\text{M}-\text{Cl}]^+$, $[\text{M}+\text{Na}]^+$ and $[\text{M}+\text{Rh}]^+$. The $^1\text{H}\{^{31}\text{P}\}$ NMR spectrum shows six singlets with equal intensity that split into pseudo-doublets in the phosphorus-coupled spectrum ($^3J_{\text{HP}} \approx 10\text{--}20$ Hz according to first-order approximation). Similarly, the $^{13}\text{C}\{^{31}\text{P}\}$ NMR spectrum shows twelve signals which substantiates the proposed symmetry of the complex. The NMR signal for the CO group could not be detected. However, its presence is evident from IR spectroscopy, which shows an intense band for the CO stretching vibration at 2007 cm^{-1} . This value is very similar to *cis*-coordinated

complexes of bis-phosphines.^{32,33} For instance, the CO stretching vibration of the bis(diphenylphosphino)ethane (dppe) complex [RhCl(dppe)(CO)] is observed at 2010 cm⁻¹.³² Therefore, the electronic properties of octaphosphine ligand **1** are comparable to classical bis-phosphines. The IR spectrum lastly also shows typical vibrations for the ^tBu group, particularly two strong bands with different intensity caused by the symmetrical deformation vibration at 1390 and 1361 cm⁻¹.

Table 1. Correlated structural (single crystal XRD) and NMR parameters (simulated ³¹P{¹H} NMR spectrum) of complex **2**.

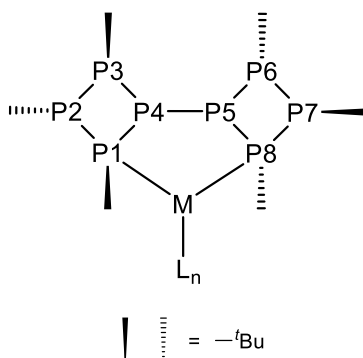
Parameter ^a	XRD	NMR ^b	
Rh1–P1	2.2475(8) Å	¹ J _{P(A)-Rh}	–163.1 Hz
Rh1–P8	2.3512(9) Å	¹ J _{P(B)-Rh}	–126.8 Hz
P–P	2.218(1) –	¹ J _{PP}	–149.0 to
	2.236(1) Å		–198.0 Hz
P4–P5	2.161(1) Å	¹ J _{P(E)-P(H)}	–318.7 Hz
Torsion (τ)	78.29(5)°	² J _{P(E)-P(G)}	+111.1 Hz
(P1-P4-P5-P8)		² J _{P(F)-P(H)}	+114.0 Hz

^aLabels for structural parameters correspond to Figure 1. ^bLabels for NMR parameters correspond to Figure 2.

Octaphosphine **1** also reacts with *cis*-[PdCl₂(cod)] (cod = 1,5-cyclooctadiene) to give the [PdCl₂(**1-κ²P²,P⁴**)] (**3**, Scheme 2). The molecular structure of complex **3** from XRD is essentially identical to complex **2** (parameters are given in Table 2; molecular structure in Figure S5, ESI; τ₄' = 0.09). This involves the same structural features, such as a shortening of the bond between the γ-P atoms as well as the tilting of the four-membered P-rings towards the metal. In addition, the dihedral angle τ (79.01(6)°) indicates a similar *gauche* conformation.

Table 2. Summary of selected structural parameters for complexes containing octaphosphine **1** in *gauche* conformation with bond lengths [Å] and angles [°].

$ML_n =$	M–P	M–L ^a	P4–P5	P–P	P1–M–P8	P–M–L ^{a,b}	τ
RhCl(CO) (2)	2.2475(8) / 2.3512(9)	1.833(6) / 2.368(1)	2.161(1)	2.218(1) - 2.236(1)	94.41(3)	92.9(2) / 90.13(4)	78.29(5)
PdCl ₂ (3)	2.270(1) / 2.274(1)	2.333(1) / 2.3444(9)	2.158(1)	2.219(1) - 2.227(1)	96.31(3)	88.38(4) / 87.66(3)	79.01(6)
Co(NO)(CO) (4)	2.233(1) - 2.240(1)	1.695(4) - 1.718(3)	2.171(2) - 2.176(2)	2.208(2) - 2.244(1)	97.15(4) - 97.17(4)	109.4(1) - 115.0(1)	92.75(7) - 93.15(6)
Pd(PPh ₃) (5)	2.3257(9) / 2.318(1)	2.309(1)	2.171(1)	2.206(1) - 2.241(1)	99.23(3)	131.49(3) - 129.20(3)	99.23(3)
CuBr (6)	2.2563(7) / 2.2644(7)	2.2919(4)	2.1979(9)	2.2110(9) 2.2244(9)	103.11(2)	125.76(2) / 131.09(2)	90.83(4)
PtCl ₂ (9)	2.2483(8) / 2.2449(8)	2.3432(8) / 2.3541(7)	2.160(1)	2.223(1) - 2.227(1)	96.03(3)	89.02(3) / 89.87(3)	74.51(5)
{AuCl} ₂ ²⁰	2.240(3) / 2.673(3)	2.334(3)	2.198(4)	2.210(4) 2.239(4)	97.7(1)	99.72(9) / 162.6(1)	100.1(2)
{AuCl} ₃ ²⁰	2.236(4) / 2.629(4)	2.323(4)	2.226(4)	2.198(5) - 2.237(5)	98.2(1)	105.5(1) / 156.4(2)	104.15(2)

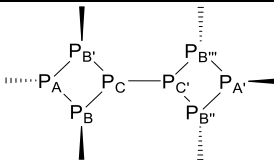
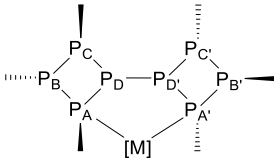


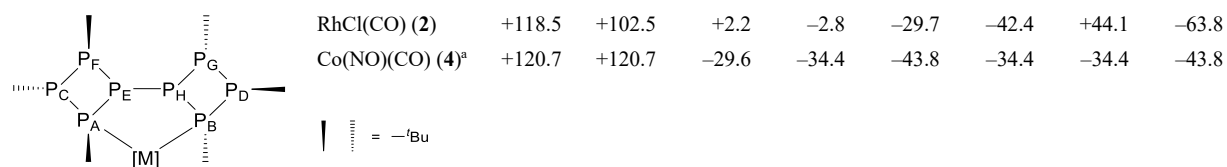
^aParameter for CO group listed first. ^bNot listed for *trans*-relation of donor atoms.

As the co-ligands in **3** are identical, the complex has C_2 symmetry. This has a large effect on the $^{31}\text{P}\{^1\text{H}\}$ NMR spectrum which shows four multiplets for pairs of chemically equivalent nuclei. However, since these nuclei are magnetically inequivalent, strong higher order effects arise resulting in very complicated multiplets. The simulation of the corresponding AA'BB'CC'DD' spin system was unsuccessful. Nevertheless, further NMR experiments confirmed the identity of the complex. The $^1\text{H}\{^{31}\text{P}\}$ NMR spectrum shows three singlets with equal intensity that split into

pseudo-doublets in the phosphorus-coupled spectrum. Similarly, the $^{13}\text{C}\{^{31}\text{P}\}$ NMR spectrum shows six signals which substantiates the proposed symmetry of the complex. The $^{31}\text{P}\{^1\text{H}\}$ - $^{31}\text{P}\{^1\text{H}\}$ COSY NMR experiment shows several cross-peaks due to the strong $^1J_{\text{PP}}$ couplings and thus reveals the connectivity within the four-membered rings. The proton-coupled ^{31}P NMR spectrum shows a significant broadening for all phosphorus atoms that are attached to ^tBu groups due to the $^3J_{\text{PH}}$ coupling ($^3J_{\text{PH}} \approx 10\text{--}20$ Hz) and therefore allow the identification of the unaffected phosphorus atoms in γ position. These observations leave two possible ways to assign the ^{31}P NMR signals to the structure of complex **3**. However, considering that the donor atoms should experience the largest low-field shift leads to one unambiguous assignment (Experimental Section). In fact, the chemical shifts of the phosphorus nuclei are in the same region as observed for the rhodium complex (Table 2). The coordinating atoms experience the largest lowfield shift ($\delta_{\text{P(A)}} +126.2$ ppm), while the signals for the γ -P atoms without ^tBu groups are observed at $\delta_{\text{P(D)}} -43.0$ ppm.

Table 2. Overview of the ^{31}P NMR chemical shifts for complexes of octaphosphine **1**.

Compound	[M] =	P _A	P _B	P _C	P _D	P _E	P _F	P _G	P _H
	– (1)	–38.3	–46.2	–103.0					
	PdCl ₂ (3)	+126.2	+10.7	–24.3	–43.0				
	Pd(PPh ₃) (5) ^a	+48.6	–26.9	–44.6	–58.2				
	CuBr (6)	–13.9	–28.1	–41.4	–76.4				
	PtCl ₂ (9)	+94.1	+7.2	–41.2	–54.0				
	AuCl ²⁰	+16.3	–39.1	–45.1	–81.5				



In addition, the IR spectrum clearly shows the presence of ^tBu groups due to their characteristic bands. Elemental analysis confirms the composition of the complex and mass spectrometry shows peaks corresponding to the ions $[M-Cl]^+$, $[M+Na]^+$ and $[M+Na+CH_3CN]^+$. Interestingly, the ions appear as a series of oxides, for instance $[PdCl(P_8^tBu_6O_x)]^+$ (x between 1 and 6) as was observed for the mass spectrum of the ligand **1**.²⁰ The hexaoxide of **1** was in fact synthesized previously.³⁶ During our study we obtained a single crystal structure thereof (more details in ESI).

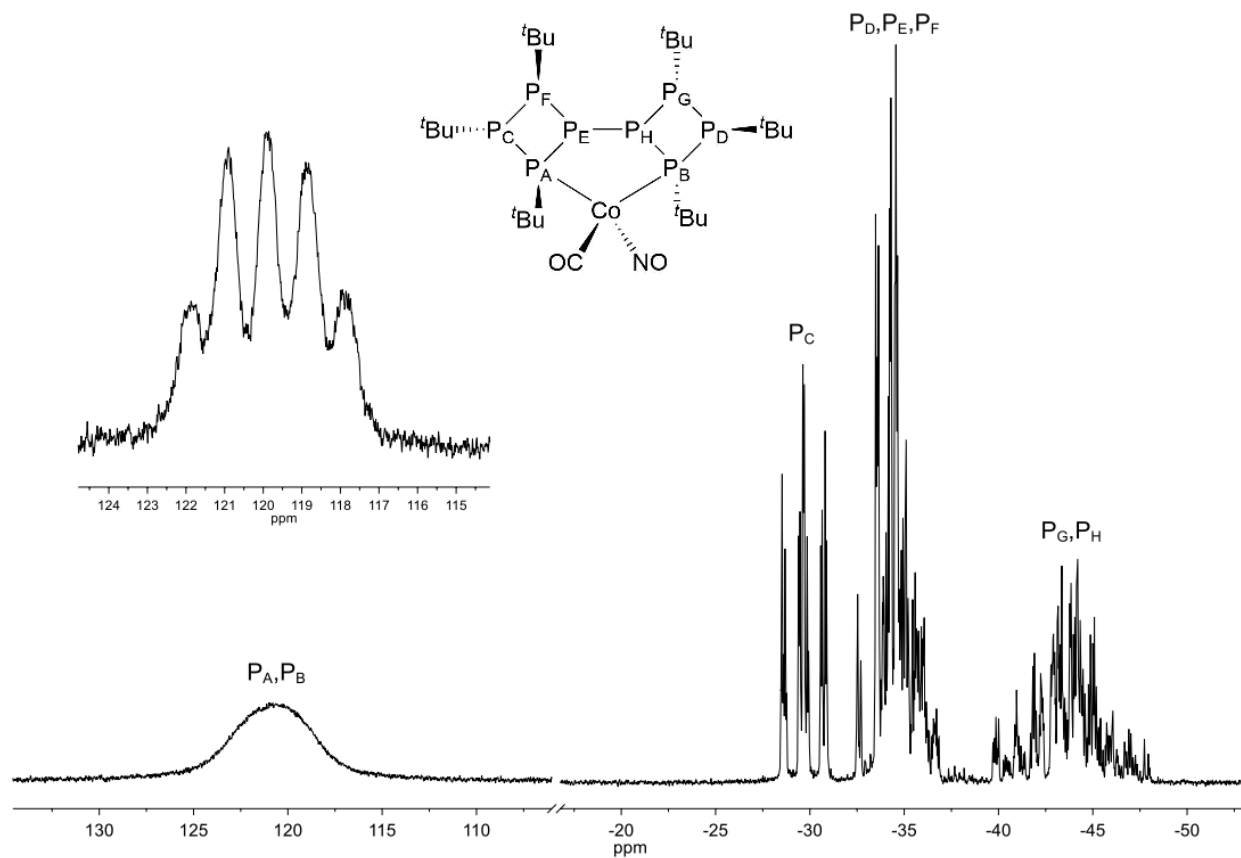


Figure 3. $^{31}\text{P}\{^1\text{H}\}$ NMR spectrum of complex **4**. The inset shows the signal $\text{P}_\text{A}/\text{P}_\text{B}$ (+120.7 ppm) at $-60\text{ }^\circ\text{C}$.

Octaphosphine **1** can also coordinate metal atoms with a tetrahedral coordination sphere ($\tau_4' = 0.93$). The reaction of **1** with one equivalent of $[\text{Co}(\text{NO})(\text{CO})_3]$ selectively gives the complex $[\text{Co}(\mathbf{1}-\kappa^2\text{P}^2, \text{P}^4)(\text{NO})(\text{CO})]$ (**4**, Scheme 2) in quantitative yield. Just as for complexes **2** and **3**, no further reaction takes place when octaphosphine **1** is treated with two or more equivalents of $[\text{Co}(\text{NO})(\text{CO})_3]$. The $^{31}\text{P}\{^1\text{H}\}$ NMR spectrum of the complex is shown in Figure 3. It consists of four distinguishable signal groups, which show a relative intensity ratio of approximately 2:1:3:2. Based on the C_1 -symmetrical structure of **4**, this intensity pattern is solely explicable with the expected ABCDEFGH spin system with overlapping multiplets. In accordance, the $^1\text{H}\{^{31}\text{P}\}$ and $^{13}\text{C}\{^1\text{H}, ^{31}\text{P}\}$ NMR spectra show six and twelve signals,

respectively, in the expected region for ^tBu groups. Furthermore, VT NMR spectroscopy shows no indication for a dynamic process giving rise to interconverting species in solution. In analogy to complexes **2** and **3**, the most shielded signals ($\delta -43.8$ ppm) correspond to the phosphorus atoms P_G and P_H in γ position. Likewise, the signals with the largest low-field shift (P_A and P_B, $\delta +120.7$ ppm) are assigned to the donor atoms coordinating at the cobalt atom. This is also in accordance with their considerable broadening ($\Delta\nu_{1/2} \approx 840$ Hz) due to the quadrupole effect of ⁵⁹Co ($I = 7/2$; NA = 100%).^{37,38} This effect is partially resolved at low temperature (inset in Figure 3), an observation that has also been made for other cobalt complexes.³⁹ Additionally, the CIS (Coordination induced shift) for P_A and P_B is furthermore comparable to these complexes.^{37,40} On the basis of these assignments, the remaining signals P_C to P_F can be assigned with the help of ³¹P{¹H}-³¹P{¹H} COSY NMR spectroscopy.

The ¹³C{¹H,³¹P} NMR signal for the carbonyl carbon atom cannot be detected, which is also likely caused by the quadrupole effect of ⁵⁹Co.^{37,38} However, the IR spectrum shows two very strong bands which arise from the stretching vibration of the CO (1948 cm⁻¹) and NO (1712 cm⁻¹) groups, besides the characteristic vibrations of the ^tBu group. These values are in excellent agreement with bis-phosphine complexes also bearing the motif {Co(bis-phosphine)(NO)(CO)}.^{37,40-42} The mass spectrum only shows signals corresponding to the ligand and its respective oxidation products which could arise from a low ionization efficiency of the cobalt complex.

Two solvomorphs of complex **4** were obtained (solvent-free and with THF). The structural parameters of both molecular structures (molecular structure in Figure S6, ESI) are almost identical and, furthermore, very similar to complexes **2** and **3** (Table 2). The main difference caused by the different coordination environment of the metal is the dihedral angle τ in the

ligand, which is approximately 10° larger (92.75(7) – 93.15(6)). Likewise, the bite angle of the octaphosphine is slightly larger (97.15(4)°) compared to **2** and **3** (94.41(3)° and 96.31(4)°). The cobalt atom is coordinated in a slightly distorted tetrahedral fashion ($\tau_4' = 0.81$). As, furthermore, the NMR spectra show no signs of paramagnetism, the cobalt thus has retained an oxidation state of –I (d^{10}). The Co–P bond lengths are slightly larger than in analogous Co complexes.^{37,38,40,43,44} Interestingly, the donor atoms of the two isoelectronic co-ligands could not be distinguished by X-ray diffraction. In fact, the best refinement for both crystal structures was achieved with a mixed site occupancy (ratio about 1:1). This is not uncommon and has also been described for similar complexes.^{38,40,44} The bond angles of the Co1–N/C–O groups deviate from linearity by approximately 10°, probably due to steric repulsion with the nearby ^tBu groups. Other bond lengths and angles fall within the normal range.^{38,43,44}

As mentioned above, phosphorus-rich metal complexes can be converted into phosphorus-rich metal phosphides by mild thermolysis.^{16,17} In order to investigate the influence of the halides we also attempted to synthesize halide-free complexes. However, reaction of complexes **2** and **3** with either lithium organyls or Grignard reagents was unsuccessful. Instead, in the latter case merely a halide exchange was achieved when using EtMgBr, resulting in the Br analogue of complex **2** (ESI). Therefore, we changed the strategy and instead used suitable precursor complexes. Reacting [Pd(PPh₃)₄] with octaphosphine **1** gives [Pd(**1**-κ²P²,P⁴)(PPh₃)] (**5**, Scheme 2) which slowly decomposes in solution. Single crystal XRD analysis of complex **5** (Figure 4, Table 2) shows that the octaphosphine adopts a *gauche* conformation. The slightly distorted trigonal-planar coordination environment at palladium(0) causes a larger bite angle of the ligand (99.23(3)°) as well as an increased dihedral angle τ (94.74(6)°). Most likely due to steric requirements, only one PPh₃ co-ligand is attached to the Pd atom. The Pd–P bond lengths for the

ligand (2.309(1) and 2.318(1) Å) are slightly larger compared to Pd^{II} complex **3** but in accordance with similar palladium(0) complexes, and thus support the proposed oxidation state.^{45–47} As for complexes **2**, **3** and **4**, a shortening of the P–P bond between the γ -P atoms occurs which seems to be a general feature of complexes of octaphosphine **1** in *gauche* conformation (Table 2). Interestingly, the trinuclear gold(I) complex [(AuCl)₃(**1**)]²⁰ is the only exception.

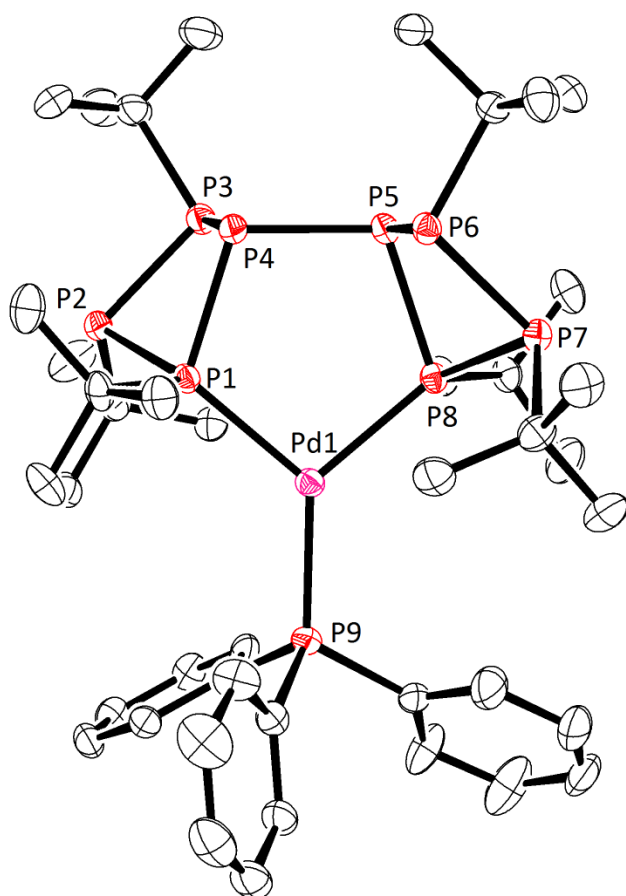
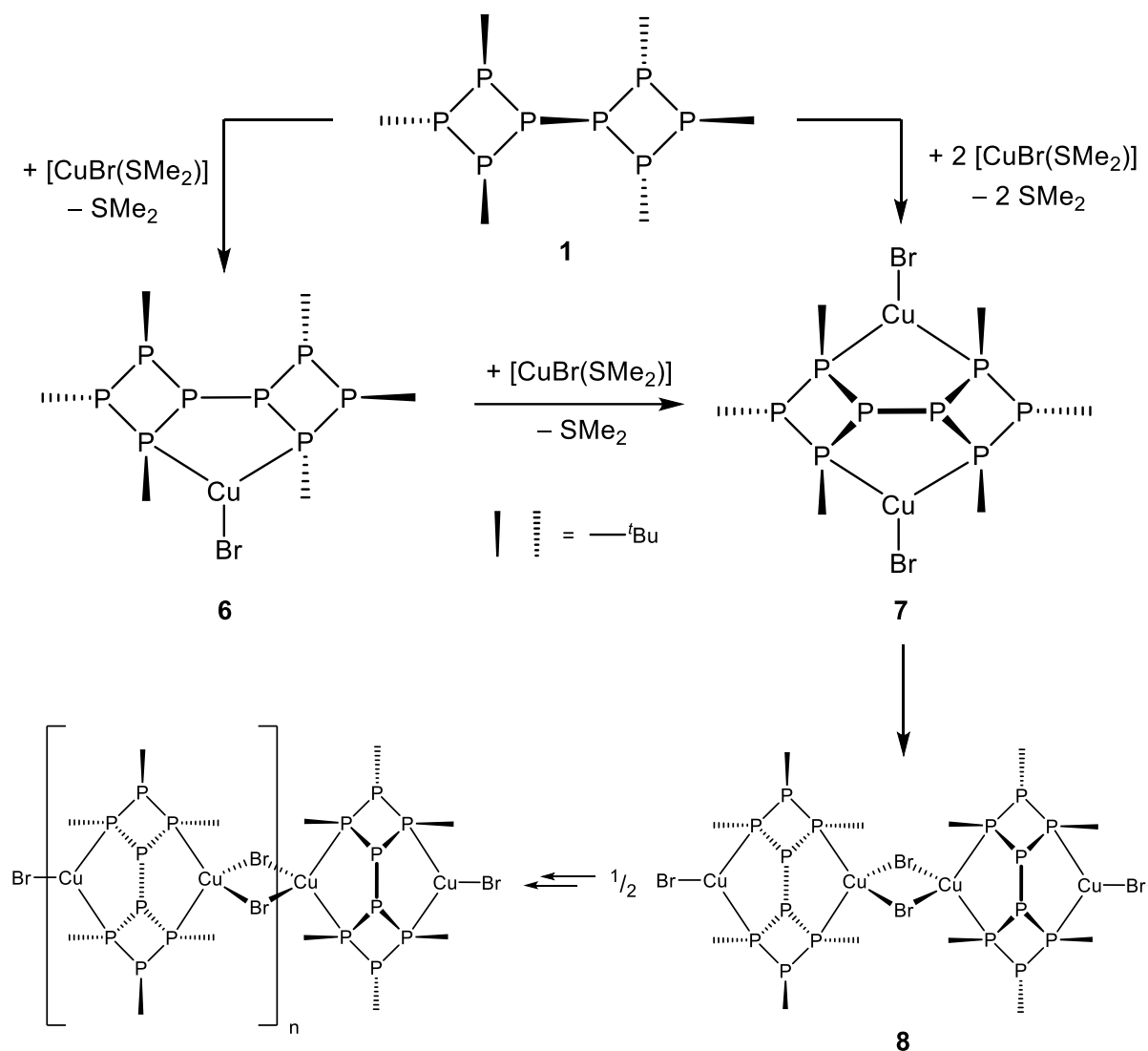


Figure 4. Molecular structure of complex **5**. Selected bond lengths [Å] and angles [°]: Pd1–P1 2.3257(9), Pd1–P8 2.318(1), Pd1–P9 2.309(1), P4–P5 2.171(1), P–P 2.206(1) - 2.241(1), P1–Pd1–P8 99.23(3), P1–Pd1–P9 131.49(3), P8–Pd1–P9 129.20(3), τ 99.23(3).

The $^{31}\text{P}\{^1\text{H}\}$ NMR spectrum of **5** consists of five multiplets which belong to an AA'BCC'DD'EE' spin system. Even though the full simulation of the spectrum was not successful, the structure in solution can be confirmed by further NMR experiments. Additional support is obtained by inspection of the fine structure of signal P_B at +23.9 ppm, which corresponds to the PPh₃ group. This signal has half relative intensity and can be well described as a first order triplet of triplets ($^2J_{\text{PP}} \approx 126$ Hz, $^3J_{\text{PP}} \approx 25$ Hz) which is in accordance with the C₂-symmetrical structure observed in the solid state. The chemical shifts of the remaining signals agree well with those observed for complexes **2-4**. The most deshielded signal P_A (δ +48.6 ppm) corresponds to the coordinating P atoms while the signal with the largest high-field shift (δ -58.2 ppm) can be assigned to the γ -P bridge atoms. Results from mass spectrometry additionally confirm the composition of the proposed complex.

As octaphosphine **1** has eight donor atoms, the formation of multinuclear complexes seems feasible, and was in fact already shown by formation of mono-, di- and trinuclear complexes with AuCl, in which two, three or four of the β -P atoms are involved in coordination.²⁰

Accordingly, by reacting **1** with [CuBr(SMe₂)], another example for a multinuclear complex was obtained. According to the number of equivalents of the copper precursor complex, either a mono- or a dinuclear complex is formed (Scheme 3). The mononuclear complex **6** is analogous to the mononuclear complexes with *gauche* conformation of the ligand, namely **2**, **3**, **4** and **5**. In contrast, the dinuclear complex **7** represents a new coordination mode for octaphosphine **1**.

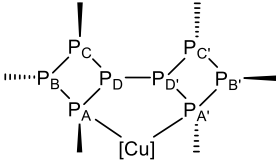
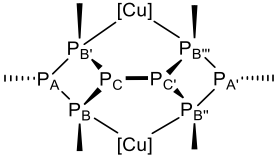



Scheme 3. Reaction of octaphosphine **1** with $[\text{CuBr}(\text{SMe}_2)]$ to give complexes **6** and **7** including dimerization to **8** as well as the proposed polymerization.

The slow addition of one equivalent of $[\text{CuBr}(\text{SMe}_2)]$ to octaphosphine **1** yields the mononuclear complex $[\text{CuBr}(\text{1-}\kappa^2\text{P}^2, \text{P}^4)]$ (**6**, Scheme 3) which according to XRD analysis is analogous to the chelate complexes **2-5** described above (Table 2). The $^{31}\text{P}\{^1\text{H}\}$ NMR spectrum of complex **6** shows four symmetrical multiplets which exhibit strong higher order effects and are therefore in good agreement with the expected AA'BB'CC'DD' spin system. As discussed for complex **2**, taking the data from $^{31}\text{P}\{^1\text{H}\}$ - $^{31}\text{P}\{^1\text{H}\}$ -COSY and the proton-coupled ^{31}P NMR spectra into

account, the signals can be assigned in two ways, with either P_A or P_C as donor atom. However, the signal P_A appears somewhat broadened, probably due to the quadrupole effect of the NMR-active copper nuclei (⁶³Cu and ⁶⁵Cu, both I = 3/2, NA = 69 and 31%). As, furthermore, in all analogous complexes with *gauche* conformation the phosphorus donor atoms are most deshielded, this signal should correspond to P_A. In fact, DFT calculations of the chemical shifts (Table 3) of complex **6** are in excellent agreement with this assignment.

Table 3. Experimental and calculated ³¹P NMR chemical shifts for the copper complexes **6** and **7**.

Complex	Signal	δ _{exp} (³¹ P)	δ _{calc} (³¹ P) ^a	CIS _{exp}
 <p style="text-align: center;">6</p>	P _A	-13.9	-17(1)	32.2
	P _B	-28.1	-34(1)	10.1
	P _C	-41.1	-38(3)	4.7
	P _D	-76.4	-76(4)	26.6
 <p style="text-align: center;">7</p>	P _A	-17.0	-18(2)	21.2
	P _B	-35.1	-31(7)	11.0
	P _C	-59.3	-40(8)	43.7
				

^aChemical shifts calculated with DFT-D3//B3LYP/def2-TVPP.

Single crystal XRD analysis shows the structural parameters of complex **6** to be very similar to analogous complexes **2-5** (Table 1). The copper atom is in a slightly distorted trigonal-planar coordination environment and, as in complexes **4** and **5**, the ligand shows an increased dihedral angle τ as well as a slightly bigger bite angle. IR spectroscopy confirms the presence of the *t*Bu groups by their characteristic vibrations. The mass spectrum shows signals corresponding to

$[\text{Cu}(\text{P}_8^t\text{Bu}_6)]^+$ including the characteristic sequence of oxides and, furthermore, weak signals relating to the ions $[\text{Cu}_2\text{Br}(\text{P}_8^t\text{Bu}_6)]^+$ and $[\text{Cu}_2\text{Br}(\text{P}_8^t\text{Bu}_6)_2]^+$.

The formation of the homodinuclear complex **7** is achieved by either slow addition of two equivalents of $[\text{CuBr}(\text{SMe}_2)]$ to octaphosphine **1** or addition of a second equivalent to the mononuclear complex **6**. In the $^{31}\text{P}\{^1\text{H}\}$ NMR spectrum of **7**, three signals with a relative intensity of 1:2:1 are observed, which is consistent with an AA'BB'B''B'''CC' spin system. Accordingly, two signals in the $^1\text{H}\{^{31}\text{P}\}$ and two sets of two signals in the $^{13}\text{C}\{^1\text{H},^{31}\text{P}\}$ NMR spectrum are observed with an intensity ratio of approximately 1:2 each. The proton-coupled ^{31}P NMR spectrum allows the identification of the P atoms with t Bu group. Considering the symmetry of the ligand, the only conceivable structure of a homodinuclear complex is thus the C_{2v} -symmetrical molecule **7** shown in Scheme 3. DFT calculations also support this assignment, even though the difference between experimental and calculated shifts are somewhat large. According to the findings from ^{31}P NMR spectroscopy, the chemical shifts of the ^{31}P nuclei show a remarkable behavior: While the coordination of a second copper atom approximately doubles the low-field shift of the atoms in α and γ position, the CIS of the donor atoms (β position) is instead reduced to 34% compared to complex **6** (Table 3), meaning they are shielded in **7** compared to the mononuclear complex. It seems likely that the conformation of the ligand is responsible for this unusual behavior.

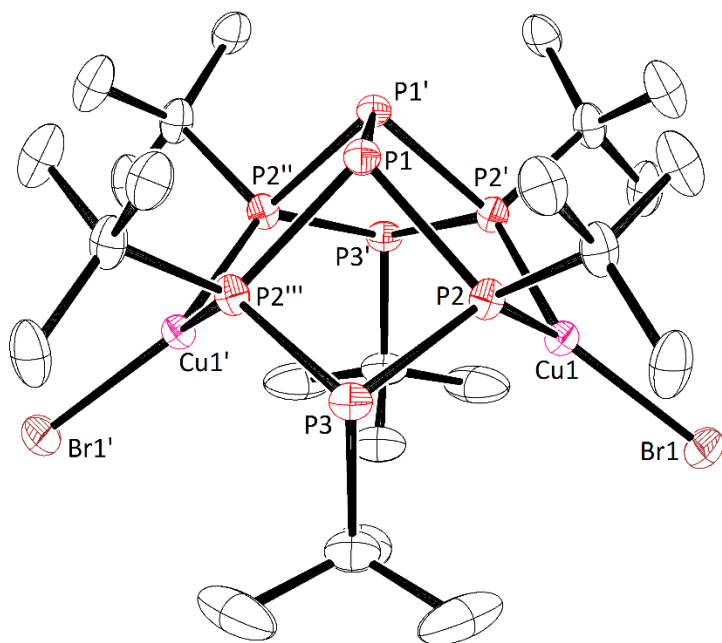


Figure 5. Molecular structure of the dinuclear complex **7**. Selected bond lengths [\AA] and angles [$^\circ$]: Cu1–P2 2.2501(6), Cu–{plane of donor atoms} 0.179(1), P1–P1' 2.248(2), P1–P2 2.2196(8), P2–P3 2.2152(8), P2–Cu1–P2' 103.13(3), Br1–Cu1–P2 127.51(2), τ 0.

In the solid state, complex **7** is located on Wyckoff-position *g* (site symmetry $2mm$, space group $P4_2/nmm$, $Z = 4$), thus representing the molecular symmetry in the crystal structure (Figure 5).

The ligand adopts the *synperiplanar* conformation ($\tau = 0^\circ$) which enables coordination to two copper(I) atoms by all four β -P atoms. In contrast to the monometallic complexes **6**, the distance between the γ -P atoms is slightly longer than for the remaining P–P bonds. The structural parameters regarding the coordination sphere of the copper atoms are very similar to those of mononuclear complex **6** involving a slightly distorted trigonal-planar coordination environment and similar bond lengths and angles. The only exception is that the Cu atom is located slightly above the plane formed by the three donor atoms. Two additional solvomorphs of the complex were crystallized which, however, show no significant difference in the structural parameters.

A DFT calculation (DFT-D3//M06L/def2-TZVP) of complexes **6** and **7** shows a complex formation energy ΔE of $-145.7 \text{ kJ}\cdot\text{mol}^{-1}$ for mononuclear complex **6** and $-83.7 \text{ kJ}\cdot\text{mol}^{-1}$ for homodinuclear complex **7** (starting from **6**). This means that the energy gained upon coordinating a metal atom ($\Delta\Delta E$) is reduced by $21.7 \text{ kJ}\cdot\text{mol}^{-1}$ for the second copper atom. This is in good agreement with the energy the octaphosphine requires for rotating from the *antiperiplanar* or *gauche* to the *synperiplanar* conformation ($\Delta G = +29.6 \text{ kJ}\cdot\text{mol}^{-1}$).

The IR spectrum of complex **7** shows the characteristic vibrations of the ^tBu groups. Mass spectrometry shows the presence of the ions $[\text{Cu}(\text{P}_8^t\text{Bu}_6)]^+$, $[\text{Cu}_2\text{Br}(\text{P}_8^t\text{Bu}_6)]^+$ and $[\text{Cu}_3\text{Br}_2(\text{P}_8^t\text{Bu}_6)]^+$. Furthermore, intense peaks are detected which can be assigned to ions of the type $[\text{Cu}_{n+1}\text{Br}_n(\text{P}_8^t\text{Bu}_6)_2]^+$ ($n = 1, 2, 3$), *i.e.* species which contain two octaphosphine ligands.

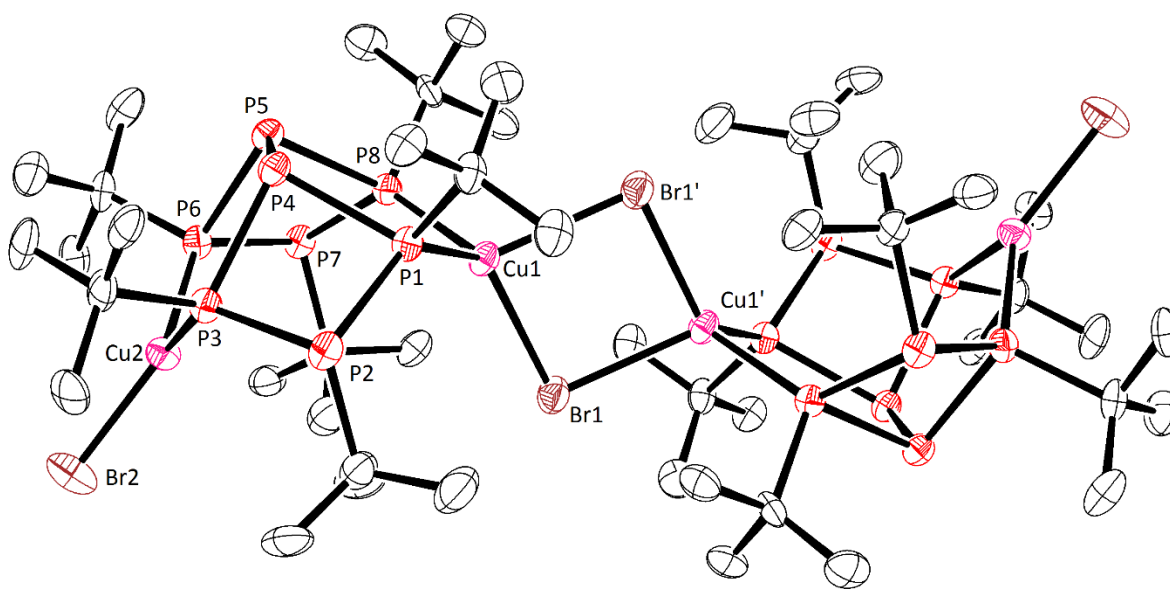
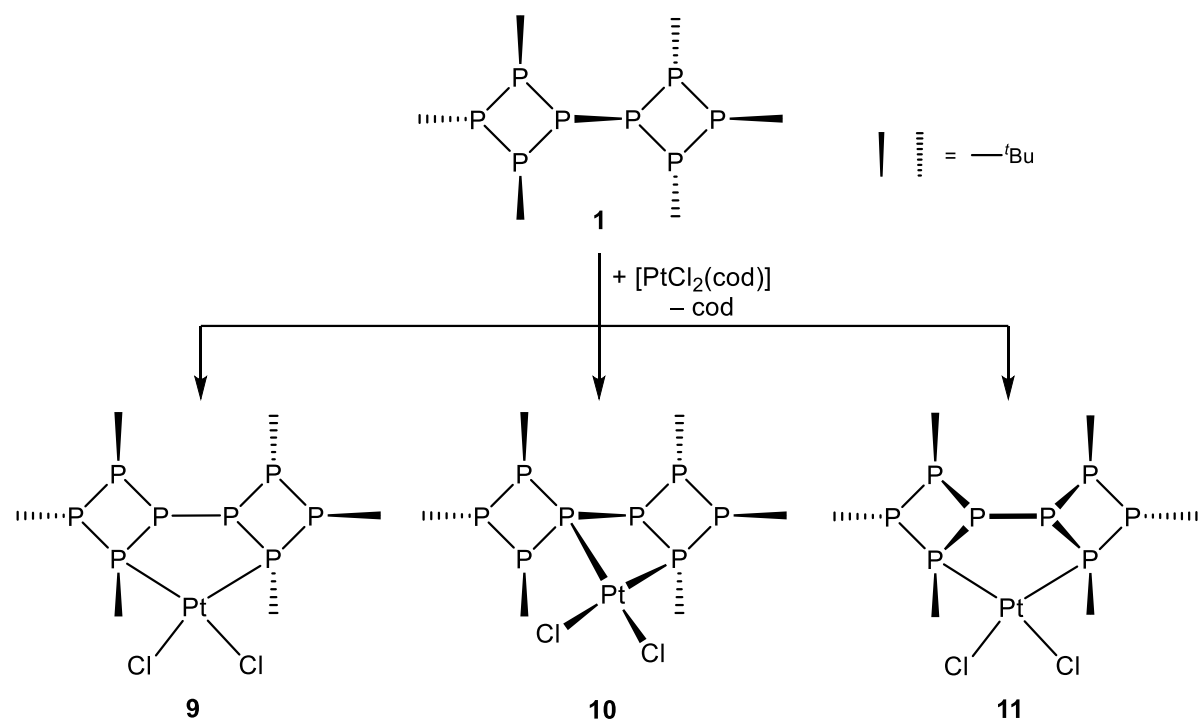


Figure 6. Molecular structure of the complex dimer **8**. Selected bond lengths [\AA] and angles [$^\circ$]: Cu1–Br1 2.469(1), Cu1–Br1' 2.534(1), Cu2–Br2 2.280(1), Cu1–P 2.321(2) - 2.316(2), Cu2–P 2.242(2) (coincid. identical), Cu2–{plane of co-ligands} 0.189, P4–P5 2.240(3), P–P 2.210(3) - 2.248(3), P1–Cu1–P8 99.78(7), P3–Cu2–P6 104.19(8), τ 1.35(1).

During the synthesis of the dinuclear copper complex **7**, small amounts of an insoluble substance were formed. The amount of this material increased, when [CuBr(SMe₂)] was rapidly added to the octaphosphine or when the reaction mixture was heated for at least one hour. From such a reaction mixture, single crystals were obtained which facilitated the elucidation of the nature of this material. The single crystal XRD analysis revealed a dimer (**8**) of the homodinuclear complex (Scheme 3, Figure 6). The two monomers are connected through two bridging bromido ions which is common for copper(I) complex.⁴⁸ The involved atom Cu1 resides in a slightly distorted tetrahedral coordination environment. The Cu1–Br bond lengths are much longer than for the terminal Cu2–Br2 bond (about 0.20–0.25 Å). As a result, the bite angle of the ligand at Cu1 (P1–Cu1–P8) is reduced by approximately 5° compared to Cu2 (P3–Cu2–P6) which is still in a trigonal-planar coordination environment. The two octaphosphine units are aligned opposite to each other. Most likely, this centrosymmetric arrangement is favored because of the steric repulsion of the ^tBu groups between the two ligands, which furthermore causes a large difference of about 0.06 Å between the two Cu1–Br bonds lengths. The remaining parameters agree with those for complexes **6** and **7**.

The dimeric complex **8** still exhibits two Cu–Br fragments in a trigonal-planar environment. It is conceivable that these fragments are capable of forming additional bromide bridges in a similar way as **7**. In fact, the dimerization energy was calculated to be –86.6 kJ·mol⁻¹, which would present a strong driving force for further oligomerization reactions given a similar energy. We therefore propose that the insoluble substance described above is a polymer and that complex **8** can be regarded as an intermediate in its formation starting from complex **7** (Scheme 3). This statement is supported by infrared spectroscopy (characteristic vibrations of the ^tBu group) and, more importantly, mass spectrometry of the insoluble material, which shows the same ions

containing one and two octaphosphine ligands **1** as observed for **6** and **7**. It should be noted that the ions of the type $[\text{Cu}_{n+1}\text{Br}_n(\text{P}_8^t\text{Bu}_6)_2]^+$ ($n = 2, 3$) which possess the distinctive feature of the oligomers ($\{\text{Cu}_2\text{Br}_2\}$ unit) are already detectable in the mass spectrum of the complexes **6** and **7**. Therefore, the oligomerization seems to take place under the ionization conditions of the MS measurement. Luminescence, which can frequently be observed for this type of bromido bridged copper(I) complexes,⁴⁸ could not be observed.



Scheme 4. Reaction of **1** with *cis*-[PtCl₂(cod)] to give the complexes **9**, **10** and the proposed complex **11**.

In all complexes discussed so far, the metal is always coordinated by the β -P atoms. However, also other P atoms in the octaphosphine can be involved in coordination, as the reaction with a platinum complex precursor shows. The reaction of octaphosphine **1** with *cis*-[PtCl₂(cod)] is less selective than for the other complexes. By optimizing this reaction, it was possible to minimize the amount of side products. In such reaction mixtures, the complex $[\text{PtCl}_2(\mathbf{1}-\kappa^2 P^2, P^4)]$ (**9**) could

be identified, which is analogous to the complexes with *gauche* conformation of the ligand, e.g. the palladium complex **3**, but furthermore also the complex $[\text{PtCl}_2(\mathbf{1}-\kappa^2P^1, P^2)]$ (**10**) which contains the octaphosphine in an *antiperiplanar* conformation coordinating the Pt atom with one of the γ -P atoms (Scheme 4). Complexes **9** and **10** thus represent linkage isomers.

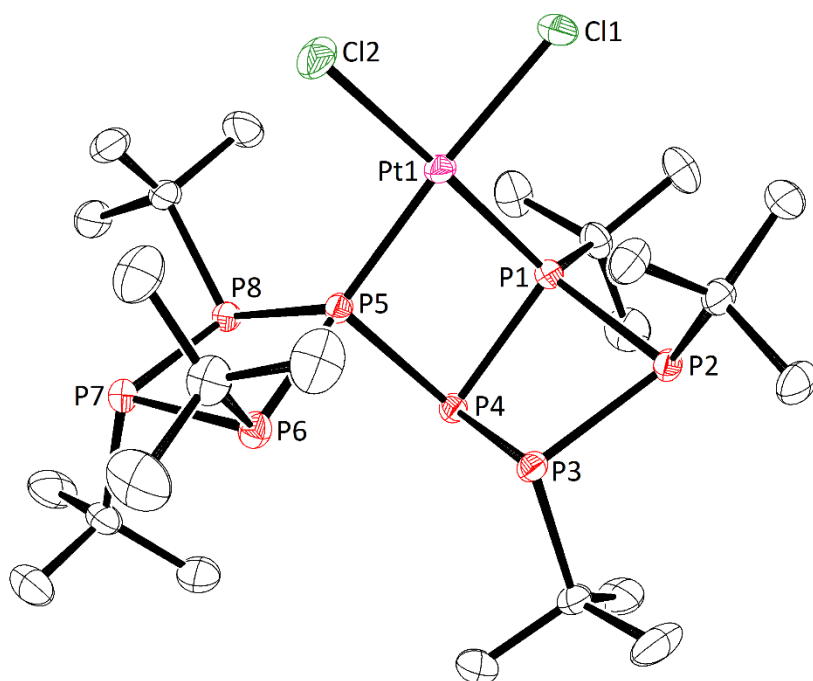


Figure 7. Molecular structure of complex **10**. Selected bond lengths [\AA] and angles [$^\circ$]: Pt1–P1 2.2411(5), Pt1–P5 2.2559(5), P1–P2 2.2006(7), P4–P5 2.2293(7), P1–Pt1–P5 80.28(2), P1–Pt1–Cl1 93.18(2), P5–Pt1–Cl2 98.06(2), τ 144.77(3).

Slow cooling of the reaction mixture gave small quantities of a mixture of crystals of **9** and **10**, suitable for single crystal XRD. While the molecular structure of complex **9** is virtually identical to the Pd^{II} complex **3**, the molecular structure of **10** (Figure 7) shows new and interesting features. In this case, instead of two β -P atoms, only one β -P atom and one γ -P atom from the other four-membered ring are coordinating the metal atom. In order to align the lone pairs of

electrons for these two phosphorus atoms, the ligand adopts a dihedral angle τ of $144.77(3)^\circ$, thus adjusting its conformation to be approximately *antiperiplanar*. The P–Pt bond lengths in **10** are 2.2559(5) Å for the γ -P atom and 2.2411(5) Å for the β -P atom carrying the *t*Bu group. This is, respectively, slightly longer and shorter than the bond lengths for the β -P atoms in complex **9** which are 2.2483(8) and 2.2449(8) Å. The platinum atom is in a slightly distorted square-planar coordination environment ($\tau_4' = 0.10$) primarily due to the small bite angle of the ligand ($80.28(2)^\circ$). In contrast to complexes with a *gauche* conformation of the octaphosphine, in **10** there is no shortening of the bond between the γ -P atoms (P4–P5), but between the coordinating β -P atom and one further atom within the ring (P1–P2).

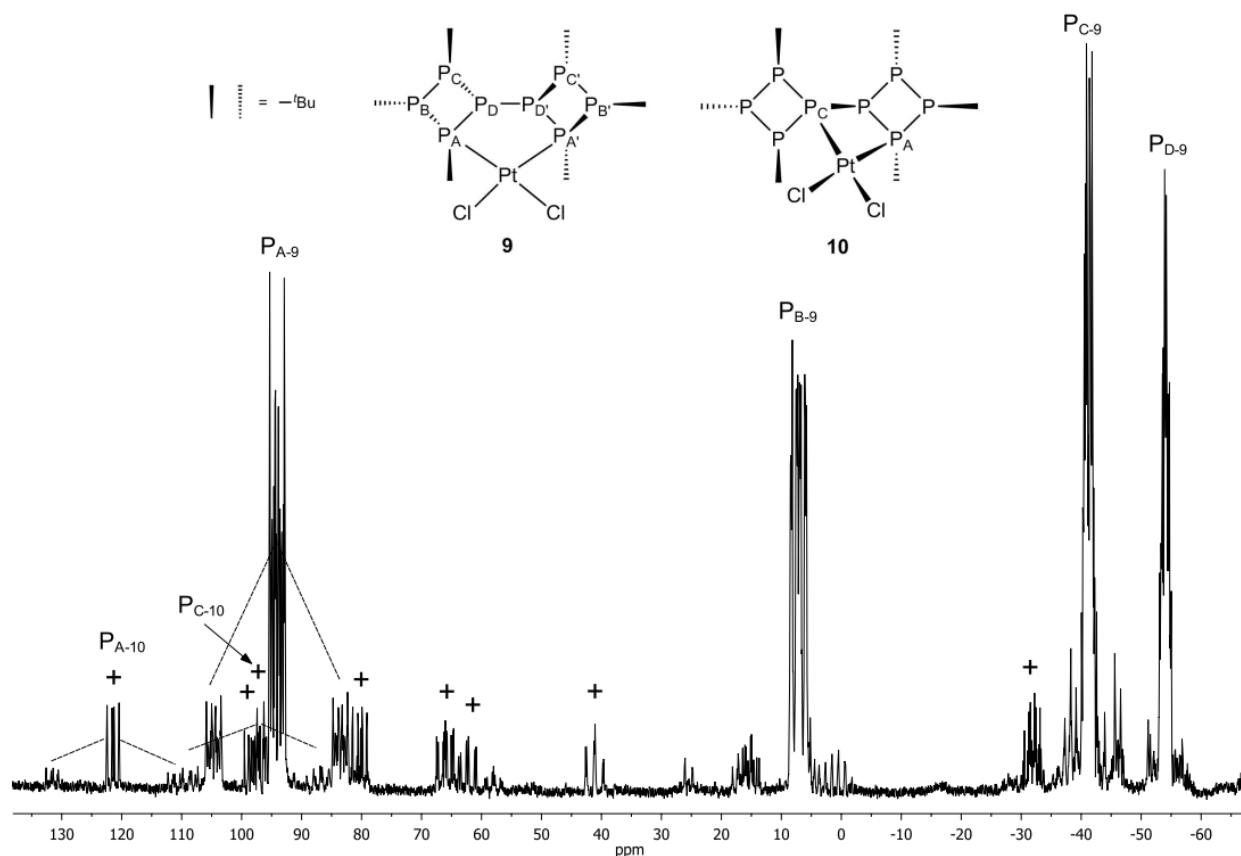


Figure 8. Section of the $^{31}\text{P}\{^1\text{H}\}$ NMR spectrum of the reaction mixture containing complexes **9**

and **10** (+). The dashed lines indicate ^{195}Pt satellites. Signals corresponding to octaphosphine **1** and unidentified signals with low intensity are also observed (at higher field, not shown here).

Complexes **9** and **10** are also observed in the $^{31}\text{P}\{^1\text{H}\}$ NMR spectrum of the reaction mixture (Figure 8). The four signals with the largest intensity can be assigned to complex **9** which is thus the major component. The chemical shifts and appearance of these ^{31}P signals strongly resemble those of palladium(II) complex **3** as the multiplets show similar higher order effects which is therefore consistent with an AA'BB'CC'DD' spin system. Furthermore, satellites (28% of total intensity) arising from a direct coupling to ^{195}Pt ($I = 1/2$, $\text{NA} = 34\%$) are observed for the most deshielded signal ($\text{P}_{\text{A-9}}$, $\delta +94.3$ ppm). The according $^1J_{\text{PPt}}$ coupling constant is approximately 3423 Hz, which is in the typical range of square-planar *cis* complexes of platinum(II).⁴⁹ Coupling constants to the other phosphorus nuclei cannot be extracted for this system. In addition to the four signals, there is a set of eight separated multiplets with only weak higher order effects, which are assigned to the ABCDEFGH spin system expected for complex **10**. Analysis of the ^{195}Pt satellites shows $^1J_{\text{PPt}}$ coupling constants of approximately 3301 Hz ($\text{P}_{\text{A-10}}$, $\delta +121.5$ ppm) and 3537 Hz ($\text{P}_{\text{C-10}}$, $\delta +97.5$ ppm). Even though a complete simulation of the spectrum was unsuccessful, the extraction of coupling constants was possible to some degree. According to this, $\text{P}_{\text{A-10}}$ shows two large P–P coupling constants ($^1J_{\text{PP}} \approx 137$ and 188 Hz) and is thus the *t*-Bu-carrying β -P donor atom, while $\text{P}_{10-\text{C}}$ is identified as the respective γ -P atom for having three large P–P coupling constants ($^1J_{\text{PP}} \approx 177$ and 2×232 Hz). The coordination-induced shift of $\text{P}_{\text{C-10}}$ ($\Delta\delta = +200.5$ ppm) is somewhat larger than for $\text{P}_{\text{A-10}}$ ($\Delta\delta = +167.6$ ppm), but a similar situation has been reported for P_7^tBu_3 and P_9^tBu_3 .^{9,50} Apparently, the CIS of P atoms only connected to other P atoms generally seems to be larger than for P atoms carrying organic

groups. Besides these two sets, there are some further, unidentified signals in the $^{31}\text{P}\{^1\text{H}\}$ NMR spectrum.

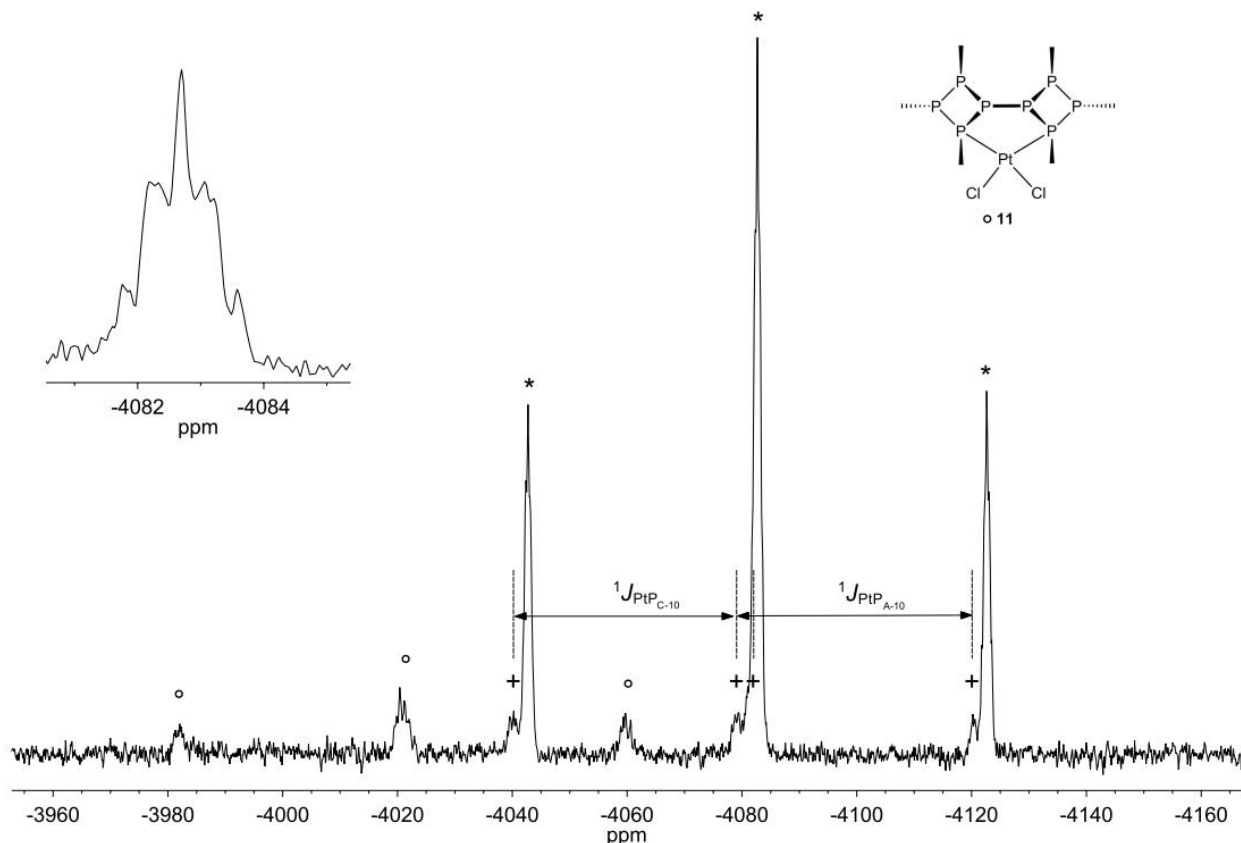


Figure 9. $^{195}\text{Pt}\{^1\text{H}\}$ NMR spectrum (85.66 MHz) of the reaction mixture containing complex **9** (*) and **10** (+) as well as proposed complex **11** (o). The inset shows a zoom of the most intense subsignal of the triplet of **9** from which long-range coupling constants could be extracted.

To support these findings, a $^{195}\text{Pt}\{^1\text{H}\}$ NMR spectrum was obtained (Figure 9), which showed three signals. The most intense signal at -4083.0 ppm shows a pseudo triplet structure ($I_{\text{rel}} \approx 1:2:1$) with a $^1J_{\text{PtP}}$ coupling constant of approximately 3423 Hz and thus corresponds to complex **9** matching the value extracted from the satellites in the $^{31}\text{P}\{^1\text{H}\}$ NMR spectrum. Interestingly, the lines of the triplet split further and allow the extraction of long-range Pt–P coupling constants ($^2J_{\text{PtPB-10}} \approx 46$ Hz, $^2J_{\text{PtPD-10}} \approx 30$ Hz,) which are two orders of magnitude smaller. The second

signal at -4080.4 ppm corresponds to complex **10**. Even though one line of this doublet of doublets is overlapped, two different coupling constants can be extracted ($^1J_{\text{PtPA-10}} \approx 3540$ Hz, $^1J_{\text{PtPC-10}} \approx 3304$ Hz) matching well those obtained from the satellites in the ^{31}P NMR spectrum. The third signal at -4020.8 ppm also shows a pseudo triplet structure ($^1J_{\text{PtP}} \approx 3328$ Hz). Reconsidering the unassigned signals in the $^{31}\text{P}\{^1\text{H}\}$ NMR spectrum, there is obviously a third platinum complex with a symmetrical bis-phosphine ligand for which the complex $[\text{PtCl}_2(\mathbf{1-}\kappa^2P^2,P^{2'})]$ (**11**) is proposed. This complex is thus a third linkage isomer, which contains octaphosphine **1** in a *synperiplanar* conformation similar to complex **7** with formal removal of one metal atom (Scheme 4), and is furthermore analogous to a rotamer of $[\text{AuCl}(\mathbf{1})]$ which was proposed to understand its dynamic behavior.²⁰ DFT calculations were carried out to support this interpretation. The relative Gibbs energies in fact show that **9** (*gauche*) represents the energetically most favored complex. The energy of **10** (*antiperiplanar*) is only slightly higher ($\Delta G_{\text{rel}}(\mathbf{10}) = +22.9$ kJ·mol⁻¹) which is consistent with the composition of the mixture. Finally, also the proposed complex **11** (*synperiplanar*) is only slightly less favored ($\Delta G_{\text{rel}}(\mathbf{11}) = +15.8$ kJ·mol⁻¹) than **9** which makes its existence conceivable.

Considering these results, it can be concluded that the $\kappa^2P^2,P^{4'}$ coordination mode (*gauche*) is most favored in complex formation with the metals reported here. The other coordination modes seem less suitable as is for instance reflected in the elongated Pt–P bond length of the γ -P atom in **10**. The reason that no analogues of complexes **10** and **11** were observed for the other metals is not due to larger relative Gibbs energies. DFT calculations showed the energies for other metals to be quite similar (Table 4). Therefore, the reason why linkage isomers could be observed for platinum(II) is most likely due to a slower substitution rate on this metal. For example, when comparing the reactivity of analogous square-planar Pd^{II} and Pt^{II} complexes, a

factor of 10^2 to 10^5 was observed.⁵¹ Therefore, other linkage isomers might also be formed for the other metals but are rapidly transformed to the energetically most favored form, which is the respective *gauche* complex.

Table 4. Relative energies^a ΔG_{rel} (in $\text{kJ}\cdot\text{mol}^{-1}$) for the different linkage isomers of the monometallic complexes.

	<i>gauche</i>	<i>antiperiplanar</i>	<i>synperiplanar</i>
PtCl ₂	0.0 (9)	+22.9 (10)	+15.8 (11)
Rh(CO)Cl ^b	0.0	+23.9	+20.8
PdCl ₂	0.0	+17.9	+17.3
Co(CO)(NO) ^b	0.0	+37.3	+9.0
PdPPh ₃	0.0	+41.4	+4.4
CuBr	0.0	+43.9	+9.3

^aCalculated with DFT-D3//M06L/def2-TVP. ^bNo significant influence of the configuration of the co-ligands was observed.

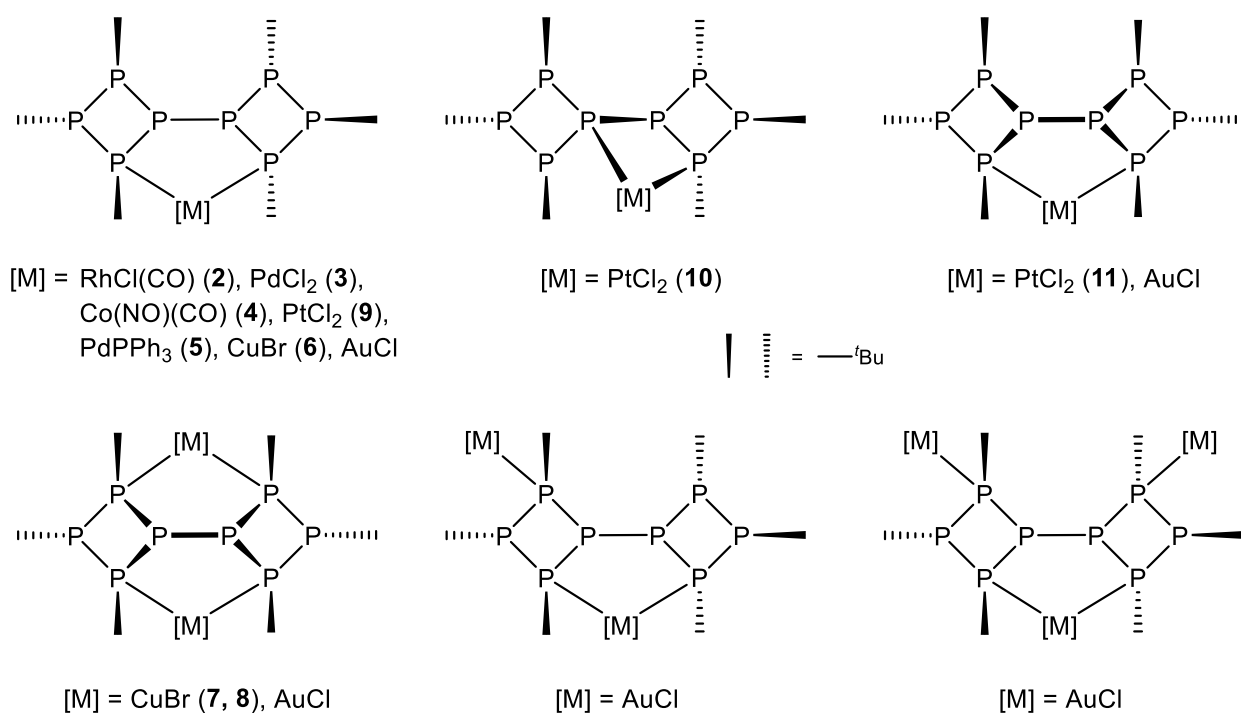
In order to test if complexes with octaphosphine **1** are suitable candidates for a conversion to phosphorus-rich metal phosphides, the thermolysis of complex **2** and **3** (toluene solvate) was investigated by thermogravimetry (TG) in combination with differential thermal analysis (DTA) as well as mass spectrometry (MS), and the residue was investigated with PXRD. The thermolysis of complex **3** occurs in three steps (Figure S5). The first step (177 °C) comprises the release of the cocrystallized toluene and, more importantly, of isobutene according to MS. Release of the latter was also observed in previous thermolysis studies of ^tBu-substituted oligophosphanide complexes.^{17,22} Interestingly, also the release of CH₃Cl is observed in this step.

This is confirmed by the similar temperature/intensity profiles (Figure S6) for $m/z = 50$ ($^{35}\text{Cl}^{12}\text{C}^1\text{H}_3^+$) and 52 ($^{37}\text{Cl}^{12}\text{C}^1\text{H}_3^+$), in combination with the intensity ratio that reflect the isotopic natural abundance of chlorine ($\text{NA}(^{35}\text{Cl}) = 75\%$, $\text{NA}(^{37}\text{Cl}) = 25\%$). This means that, apparently, the ^tBu groups are not only released as isobutene (C_4H_8) and hydrogen but also as smaller hydrocarbon fragments. This, in turn, enables a possible liberation for the chloride anions coordinated at the metal atom and could thus avoid contamination of the metal phosphide with halides. Between steps 1 and 2 as well as between 2 and 3, a plateau is observed which indicates formation of stable intermediates. For step 2 ($447\text{ }^\circ\text{C}$), no species could be identified. In step 3 ($814\text{ }^\circ\text{C}$), white phosphorus (P_4) is liberated at last, which is also in accordance with previous studies. Remarkably, the high onset temperature of this step enables a wide temperature range for the selective conversion avoiding the release of P_4 . The PXRD of the residue shows reflections that cannot be assigned to any known palladium phosphide phase or the single elements and thus points to a new material. The composition of the remaining solid, assuming no metal loss, would be $\text{PdP}_{8.5}$. Besides the fact that the release of P_4 was observed, elements other than Pd and P must be present as the amount of phosphorus in this case exceeds the ratio of the starting material ($\text{P}:\text{Pd} = 8$).

The Rh^{I} complex **2** is also decomposed in three steps (Figure S7). While the species released in step 1 ($172\text{ }^\circ\text{C}$) could not be assigned, the second step ($261\text{ }^\circ\text{C}$) involves the cleavage of the Cl, CO as well as ^tBu groups. In analogy to complex **3**, liberation of isobutene and CH_3Cl are observed. Interestingly, CO is not only released as the free gas but also in the form of CO_2 and hydrogenation products, such as formaldehyde CH_2O and apparently even CH_4 . Step 3 ($512\text{ }^\circ\text{C}$) occurs at much higher temperature and again involves the release of P_4 but also $\text{C}_2\text{H}_5\text{Cl}$. The

remaining phase, according to the mass losses, is calculated to be RhP_3 . However, PXRD (Figure S8) shows that this material contains the phosphorus-rich rhodium phosphide RhP_2 .⁵²

In summary, the investigated complexes release the $t\text{Bu}$ groups in form of isobutene at relatively low temperatures. This also involves the co-ligands including the halide atoms which are released in the form of organohalides. White phosphorus is released at much higher temperatures. Even though these are just preliminary investigations, these results show the potential of transition metal complexes of octaphosphine **1** as precursors for phosphorus-rich metal phosphides.



Scheme 5. Overview of the coordination modes of octaphosphine **1**. Complexes with [M] = AuCl taken from literature²⁰.

Conclusion. Including the gold(I) complexes reported previously,²⁰ six different coordination modes involving mono-, di- as well as trinuclear complexes with octaphosphine **1** have been observed so far (Scheme 5). The predominant form is the monometallic chelate complex

[MLL'(1- κ^2 P²,P^{4'})], in which the octaphosphine ligand adopts a *gauche* conformation. Several complexes of this kind were obtained including metal atoms in square-planar (M = Rh^I, L = CO with L' = Cl (**2**), M = Pd^{II}, L = L' = Cl (**3**), M = Pt^{II}, L = L' = Cl (**9**)), and tetrahedral coordination environment (M = Co^{-I}, L = NO, L' = CO (**4**)) as well as trigonal-planar complexes [ML(1- κ^2 P²,P^{4'})] (M = Pd⁰, L = PPh₃ (**5**); M = Cu^I, L = Br (**6**); M = Au^I, L = Cl²⁰). The reaction with *cis*-[PtCl₂(cod)] allowed identification of two further coordination modes. In one, a γ -P atom is involved in coordination which requires an *antiperiplanar* conformation of the ligand (**10**), in the second, again two of the β -P atoms coordinate but with the ligand in a *synperiplanar* conformation (**7**, **8**, **11**). These results show that octaphosphine **1** in fact exhibits a highly versatile coordination chemistry. Even though the molecule is relatively rigid, it still allows adjustment of structural parameters, especially the rotation around the internal P–P bond, to enable coordination of the different metals. Finally, thermolysis of selected complexes shows them to be suitable precursors for phosphorus-rich materials.

Experimental Section. All experiments were carried out under nitrogen using standard Schlenk techniques. Toluene, dichloromethane, diethyl ether, pentanes as well as hexanes (isomeric mixtures) and acetonitrile were dried and degassed with an MB SPS-800 Solvent Purification System (MBRAUN) and kept over molecular sieves (4 Å). THF was distilled from potassium and benzophenone and kept over molecular sieves (4 Å). The compounds {*cyclo*-(P^{4'}Bu₃)₂}₂ (**1**)²⁰, [RhCl(CO)₂]₂⁵³, and [CuBr(SMe₂)]₂⁵⁴ were prepared as described in the literature. All other chemicals were purchased and used without further purification. Luminescence was tested with a common laboratory UV lamp at 254 and 365 nm.

NMR Spectroscopy. NMR spectra were recorded at 25 °C with a BRUKER AVANCE DRX 400 spectrometer (¹H NMR: 400.13 MHz, ¹³C NMR: 100.16 MHz, ³¹P NMR: 161.97 MHz) or a

Bruker Avance III HD 400 spectrometer (^{195}Pt NMR: 85.66 MHz). TMS was used as internal standard for ^1H NMR spectroscopy. ^{13}C and ^{31}P NMR experiments were referenced to the Ξ scale.⁵⁵ Every signal labeling in this publication also extends to the chemically equivalent yet magnetically nonequivalent nuclei *i.e.* P_A for P_A , P_A' as well as P_A'' and so forth. The ^{31}P NMR signals are labeled alphabetically starting from the nucleus which is most deshielded, with the exceptions of complex **5** for the sake of clarity (Table 2). All ^{31}P NMR spectra were measured with a 90° pulse and reduced acquisition (0.6 s) as well as d1 time (1.0 s). At least 1000 scans were necessary to obtain acceptable spectra. The samples were usually saturated solutions of the respective compound. Suitable spectra for simulation required about 100,000 scans. Simulation of the NMR spectra was performed using the DAISY module implemented in the program TopSpin version 3.6.1 (BRUKER, BioSpin GmbH, Rheinstetten). For this, the $^1J_{\text{PP}}$ coupling constants were set negative.⁵⁶

X-Ray Crystallography. Single crystal X-ray diffraction data were collected with a GEMINI CCD diffractometer (RIGAKU). The radiation source was a molybdenum anode (Mo-K_α , $\lambda = 0.71073 \text{ \AA}$). The absorption corrections were carried out semiempirically with the SCALE3 ABSPACK module.⁵⁷ All structures were solved by dual space methods with Sir-92.⁵⁸ Structure refinement was done with SHELXL-2015⁵⁹ by using full-matrix least-square routines against F^2 . All hydrogen atoms were calculated on idealized positions. The pictures were generated with the program ORTEP3.⁶⁰ In all pictures, hydrogen atoms, disorders and solvent molecules were omitted for clarity and thermal ellipsoids are shown with 50% probability. Powder X-ray diffraction data were collected on a STADI-P diffractometer (STOE) with a silicon solid-state detector Methyn-1K (DECTRIS) at room temperature. The radiation source was a copper anode (Cu-K_α , $\lambda = 1.540598 \text{ \AA}$) combined with a germanium single crystal monochromator. Samples

were measured in sealed glass capillaries (inner diameter 0.5 mm, HILGENBERG) with Debye-Scherrer geometry. Processing of the raw data was carried out with the diffractometer software WinXPow⁶¹ (STOE). The phase analysis was carried out based on the PDF-2 database (ICDD). The Rietveld analysis for complex **2** was performed with a fundamental parameter approach using the software TOPAS⁶² (BRUKER). In this case, only the unit cell dimensions were refined, retaining the original space group and structural parameters of the molecule. The new cell dimensions for the crystal structure of complex **2** were $a = 17.653(5) \text{ \AA}$, $b = 11.582(3) \text{ \AA}$, $c = 18.569(3) \text{ \AA}$, $\beta = 97.069(9)^\circ$ and $V = 3767.8(18) \text{ \AA}^3$.

Other Physical Measurements. A VARIO EL (HERAEUS) microanalyzer was used to determine the elemental composition of the compounds. Samples for IR spectroscopy were prepared as KBr pellets in a nitrogen-filled glove box and the spectra were recorded in the range of $400 - 4000 \text{ cm}^{-1}$ using a PERKINELMER (System 2000) FT-IR spectrometer. Mass spectrometry measurements were carried out as ESI-MS with a BRUKER DALTONICS FT-ICR-MS spectrometer (Type APEX II, 7 Tesla). The thermal analyses were carried out as TG and DTA coupled with MS under dynamic argon atmosphere using a NETZSCH STA449F1 thermoanalyzer connected with a NETZSCH QMS-403C AEOLOS mass spectrometer (heating rate $10 \text{ }^\circ\text{C}\cdot\text{min}^{-1}$, flow rate $25 \text{ mL}\cdot\text{min}^{-1}$, Al_2O_3 crucibles, mass of sample approximately 20 mg, temperature range $25 - 900 \text{ }^\circ\text{C}$). After the experiment, the sample was transferred to a glass capillary under nitrogen for further analysis with PXRD.

Quantum Chemical Calculations. All calculations were carried out with DFT using the program ORCA⁶³ (version 3.0.2). For all calculations, the convergence criterion was increased to 10^{-8} Hartree, the atom-pairwise dispersion correction D3^{64,65} was used and a simulation of the solvent environment was performed using the COSMO⁶⁶ model for which the dielectric constant

was set to 7.58 (THF). Relativistic effects were considered using effective core potentials^{67,68}. Furthermore, the RIJCOSX approximation was used to speed up the calculations. To find the best combination of functional and basis set for the energies of the complexes of octaphosphine **1**, a benchmarking study was carried out based on the CO stretching vibration of the Rh^I complex **2** by performing a frequency analysis. Due to the best agreement with the experimental value ($\Delta\nu = 12 \text{ cm}^{-1}$, Table S2, ESI), the M06L functional⁶⁹ in combination with the def2-TZVP^{70,71} basis set was used for geometry optimization of the molecular geometries as well as the according energies including numerical frequency analysis. The ³¹P NMR chemical shifts were calculated with the B3LYP functional^{72,73} in combination with the def2-TZVPP basis set.

Synthesis of [RhCl(CO)(1- κ^2 P²,P⁴)] (2**).** A solution of octaphosphine **1** (105 mg, 0.178 mmol, 1.0 eq) in 7 mL toluene was added to [$\{\text{RhCl}(\text{CO})_2\}_2$] (42 mg, 0.216 mmol, 1.2 eq of Rh). Upon stirring the solution turned dark brown and gas evolution was observed. The reaction mixture was warmed to 60 °C for six hours. Evaporation of the solvent under reduced pressure gave a solid which was extracted with two times 7 mL toluene. Removal of the solvent of the combined phases under reduced pressure and drying under vacuum for 30 min gave a brown crystalline powder (108 mg, 80%). Additional information in ESI. ¹H{³¹P} NMR (C₆D₆): $\delta = 1.60$ (s, 9H, CH₃), 1.54 (s, 9H, CH₃), 1.50 (s, 9H, CH₃), 1.47 (s, 9H, CH₃), 1.28 (s, 9H, CH₃), 1.25 (s, 9H, CH₃) ppm. ¹³C{¹H,³¹P} NMR (C₆D₆): $\delta = 37.8$ (s, C-P), 33.5 (s, C-P), 33.2 (s, C-P), 30.6 (s, C-P), 30.1 (s, C-P), 29.5 (s, C-P), 29.1 (s, CH₃), 28.3 (s, CH₃), 28.1 (s, CH₃), 27.8 (s, CH₃), 26.6 (s, CH₃), 20.2 (s, CH₃) ppm. (The carbonyl signal could not be detected.) ³¹P{¹H} NMR (C₆D₆): ABCDEFGHX spin system (R = 1.214%) $\delta = 118.49$ (P_A), 102.55 (P_B), 2.17 (P_C), -2.81 (P_D), -29.72 (P_E), -42.44 (P_F), -44.08 (P_G), -63.78 (P_H) ppm. ²J_{AB} = -4.43, ¹J_{AC} = -198.02, ³J_{AD} = 0.02, ¹J_{AE} = -175.36, ²J_{AF} = +24.61, ³J_{AG} = -0.37, ²J_{AH} = +4.18, ¹J_{AX} = -163.09, ³J_{BC} = +0.90, ¹J_{BD} = -

195.04, $^2J_{BE} = +6.08$, $^3J_{BF} = -0.32$, $^2J_{BG} = +22.44$, $^1J_{BH} = -162.59$, $^1J_{BX} = -126.82$, $^4J_{CD} = +1.52$, $^2J_{CE} = +43.22$, $^1J_{CF} = -152.18$, $^2J_{CG} = +1.00$, $^4J_{CH} = -12.14$, $^2J_{CX} = 0.00$, $^3J_{DE} = -14.26$, $^4J_{DF} = +1.05$, $^1J_{DG} = -149.04$, $^2J_{DH} = +44.87$, $^2J_{DX} = 0.00$, $^1J_{EF} = -187.59$, $^2J_{EG} = +114.03$, $^1J_{EH} = -318.68$, $^2J_{EX} = 0.00$, $^3J_{FG} = +23.81$, $^2J_{FH} = +111.13$, $^3J_{FX} = 0.00$, $^1J_{GH} = -179.97$, $^3J_{GX} = 0.00$, $^2J_{HX} = 0.00$ Hz. IR (KBr): $\tilde{\nu} = 3859$ (w), 3677 (w), 3437 (m), 2944 (s, $\nu_{\text{as}}(\text{C-H})$), 2890 (s, $\nu_{\text{s}}(\text{C-H})$), 2855 (s, $\nu_{\text{s}}(\text{C-H})$), 2007 (s, $\nu(\text{C-O})$), 1992 (m, $\nu(\text{C-O})$), 1631 (m), 1458 (s, $\delta_{\text{as}}(\text{CH}_3)$), 1390 (m, $\delta_{\text{s}}(\text{CH}_3)$), 1361 (s, $\delta_{\text{s}}(\text{CH}_3)$), 1170 (s, $\rho(\text{CH}_3) + \nu_{\text{s}}(\text{C-C})$), 1014 (m, $\rho(\text{CH}_3)$), 937 (w, $\rho(\text{CH}_3) + \nu_{\text{s}}(\text{C-C})$), 803 (m, $\nu_{\text{s}}(\text{C-C})$), 578 (w), 534 (w), 505 (w), 459 (w) cm^{-1} . MS (ESI(+), MeCN): $m/z = 693.1$ [LRh]⁺ (100%), 709.1 [LRhO]⁺ (5%), 721.1 [LRh(CO)]⁺ (46%), 807.0 [LRh(CO)O]⁺ (1%), 779.1 [LRhCl(CO)Na]⁺ (1%), 791.0 [LRhCl(CO)NaO]⁺ (1%), 859.0 [LRhCl(CO)Rh]⁺ (2%). L = C₂₄H₅₄P₈. MP: 302 °C. EA (%) for C₂₅H₅₄ORhClP₈; calc. C 39.67, H 7.19; found C 39.16, H 7.14.

Synthesis of [PdCl₂(1- κ^2 P²,P⁴)](3). A solution of octaphosphine **1** (136 mg, 0.230 mmol, 1.0 eq) in 8 mL toluene was added to *cis*-[PdCl₂(cod)] (90 mg, 0.315 mmol, 1.4 eq). The reaction mixture was heated under reflux for 15 hours. Evaporation of the solvent under reduced pressure gave an orange solid which was extracted with four times 10 mL Et₂O. Removal of the solvent of the combined phases under reduced pressure and drying under vacuum for 30 min gave a brown powder (175 mg, 99%). ¹H{³¹P} NMR (C₆D₆): $\delta = 1.77$ (s, 18H, (H₃C)₃C-P_A), 1.58 (s, 18H, (H₃C)₃C-P_B), 1.03 (s, 18H, (H₃C)₃C-P_C) ppm. ¹³C{¹H,³¹P} NMR (C₆D₆): $\delta = 41.0$ (s, C-P_A), 35.6 (s, C-P_B), 30.6 (s, C-P_C), 30.4 (s, (H₃C)₃C-CP_A), 29.9 (s, (H₃C)₃C-CP_B), 28.5 (s, (H₃C)₃C-CP_C) ppm. ³¹P{¹H} NMR (C₆D₆): $\delta = 162.2$ (m, 2P, P_A), 10.7 (m, 2P, P_B) -24.3 (m, 2P, P_C), -43.0 (m, 2P, P_D) ppm. IR (KBr): $\tilde{\nu} = 3855$ (w), 3747 (w), 3673 (w), 3651 (w), 2947 (s, $\nu_{\text{as}}(\text{C-H})$), 2891 (s, $\nu_{\text{s}}(\text{C-H})$), 2859 (s, $\nu_{\text{s}}(\text{C-H})$), 2006 (w), 1702 (w), 1495 (w), 1458 (s, $\delta_{\text{as}}(\text{CH}_3)$), 1391 (m,

$\delta_s(\text{CH}_3)$), 1362 (s, $\delta_s(\text{CH}_3)$), 1261 (w), 1168 (s, $\rho(\text{CH}_3) + \nu_s(\text{C}-\text{C})$), 1013 (m, $\rho(\text{CH}_3)$), 936 (m, $\rho(\text{CH}_3) + \nu_s(\text{C}-\text{C})$), 803 (m, $\nu_s(\text{C}-\text{C})$), 728 (w), 694 (w), 624 (w), 530 (w), 463 (w), 421 (w) cm^{-1} . MS (ESI(+), MeCN): L = $\text{C}_{24}\text{H}_{54}\text{P}_8$ $m/z = 733.1$ [LPdCl] $^+$ (100%), 749.1 [LPdClO] $^+$ (9%), 791.0 [LPdNaCl_2] $^+$ (11%), 807.0 [$\text{LPdNaCl}_2\text{O}$] $^+$ (3%), 830.1 [$\text{LPd}(\text{MeCN})\text{NaCl}_2$] $^+$ (57%), 846.0 [$\text{LPd}(\text{MeCN})\text{NaCl}_2\text{O}$] $^+$ (6%), 1465.2 [$\text{L}_2\text{Pd}_2\text{Cl}_2$] $^+$ (12%), 1481.2 [$\text{L}_2\text{Pd}_2\text{Cl}_2\text{O}$] $^+$ (3%), 1499.2 [$\text{L}_2\text{Pd}_2\text{Cl}_2\text{O}_2$] $^+$ (1%). MP: 198 °C. EA (%) for $\text{C}_{24}\text{H}_{54}\text{PdCl}_2\text{P}_8$; calc. C 37.54, H 7.09; found C 37.32, H 7.00.

Synthesis of $[\text{Co}(\text{NO})(\text{CO})(1-\kappa^2\text{P}^2, \text{P}^4)]$ (4). A solution of $[\text{Co}(\text{NO})(\text{CO})_3]$ (0.231 mmol, 1.4 eq) in THF was added to a solution of octaphosphine **1** (93 mg, 0.158 mmol, 1.0 eq) in 10 mL THF. The reaction mixture was warmed to 60 °C for 24 hours. Evaporation of the solvent under reduced pressure and drying under vacuum gave a bronze powder (113 mg, 99%). Single crystals of the solvent-free solvomorph were obtained by slowly passing a stream of nitrogen over a THF solution. Single crystals of the THF solvomorph were obtained from a THF solution at -30 °C. $^1\text{H}\{^{31}\text{P}\}$ NMR (THF- d_8): $\delta = 1.38$ (s, 9H, $(\text{H}_3\text{C})_3\text{C-P}_A$), 1.30 (s, 18H, $(\text{H}_3\text{C})_3\text{C-P}_B/\text{P}_C$), 1.26 (s, 9H, $(\text{H}_3\text{C})_3\text{C-P}_D$), 1.25 (s, 9H, $(\text{H}_3\text{C})_3\text{C-P}_E$), 1.20 (s, 9H, $(\text{H}_3\text{C})_3\text{C-P}_F$) ppm. $^{13}\text{C}\{^1\text{H}, ^{31}\text{P}\}$ NMR (THF- d_8): $\delta = 37.3$ (s, C-P), 35.9 (s, C-P), 30.6 (s, C-P), 30.5 (s, C-P), 30.2 (s, C-P), 29.7 (s, C-P), 29.4 (s, CH_3), 28.6 (s, CH_3), 27.6 (s, CH_3), 27.5 (s, CH_3), 27.2 (s, CH_3), 27.0 (s, CH_3) ppm. (The carbonyl signal could not be detected.) $^{31}\text{P}\{^1\text{H}\}$ NMR (THF- d_8 , 25 °C): $\delta = 120.7$ (m, 2P, P_A/P_B), -29.6 (m, 1P, P_C), -34.4 (m, 3P, $\text{P}_D/\text{P}_E/\text{P}_F$), -43.8 (m, 2P, P_G/P_H) ppm. $^{31}\text{P}\{^1\text{H}\}$ NMR (THF- d_8 , -60 °C): $\delta = 119.9$ (m, 2P, P_A/P_B), -38.7 (m, 4P, $\text{P}_C/\text{P}_D/\text{P}_E/\text{P}_F$), -47.1 (m, 2P, P_G/P_H) ppm. IR (KBr): $\tilde{\nu} = 3888$ (w), 3872 (w), 2993 (w), 2949 (s, $\nu_{\text{as}}(\text{C}-\text{H})$), 2890 (s, $\nu_s(\text{C}-\text{H})$), 2855 (s, $\nu_s(\text{C}-\text{H})$), 1948 (s, $\nu(\text{C}-\text{O})$), 1712 (s, $\nu(\text{N}-\text{O})$), 1495 (w), 1469 (w), 1455 (s, $\delta_{\text{as}}(\text{CH}_3)$), 1388 (m, $\delta_s(\text{CH}_3)$), 1360 (s, $\delta_s(\text{CH}_3)$), 1261 (w), 1171 (s, $\rho(\text{CH}_3) + \nu_s(\text{C}-\text{C})$), 1009 (m, $\rho(\text{CH}_3)$), 938 (w,

$\rho(\text{CH}_3) + \nu_s(\text{C}-\text{C})$), 802 (m, $\nu_s(\text{C}-\text{C})$), 617 (w), 572 (w), 499 (s), 454 (w), 413 (w) cm^{-1} . MS (ESI(+), MeCN/THF 1:1): $m/z = 607.2$ $[\text{LOH}]^+$ (13%), 623.2 $[\text{LO}_2\text{H}]^+$ (62%), 629.2 $[\text{LONa}]^+$ (10%), 639.2 $[\text{LO}_3\text{H}]^+$ (13%), 645.2 $[\text{LO}_2\text{Na}]^+$ (100%), 655.2 $[\text{LO}_4\text{H}]^+$ (2%), 661.2 $[\text{LO}_3\text{Na}]^+$ (37%), 671.2 $[\text{LO}_5\text{H}]^+$ (4%), 677.2 $[\text{LO}_4\text{Na}]^+$ (5%), 1251.4 $[(\text{P}_8^t\text{Bu}_6)_2\text{O}_3\text{Na}]^+$ (7%), 1267.4 $[(\text{P}_8^t\text{Bu}_6)_2\text{O}_4\text{Na}]^+$ (34%), 1283.4 $[(\text{P}_8^t\text{Bu}_6)_2\text{O}_5\text{Na}]^+$ (12%), 1299.4 $[(\text{P}_8^t\text{Bu}_6)_2\text{O}_6\text{Na}]^+$ (2%). L = $\text{C}_{24}\text{H}_{54}\text{P}_8$. MP: 252 °C. EA (%) for $\text{C}_{25}\text{H}_{54}\text{NO}_2\text{CoP}_8$; calc. C 42.45, H 7.69, N 1.98; found C 42.14, H 7.39, N 1.89.

Synthesis of $[\text{Pd}(\text{PPh}_3)(1-\kappa^2\text{P}^2, \text{P}^4)]$ (5**).** 7 mL THF were added to mixture of octaphosphine **1** (175 mg, 0.298 mmol, 1.0 eq) and $[\text{Pd}(\text{PPh}_3)_4]$ (344 mg, 0.297 mmol, 1.0 eq). Upon stirring, the initial suspension became a clear deep brown solution within minutes. The solution was stirred for two hours and then kept for crystallization at -30 °C. Clear orange crystals of **5** were obtained after 2 d (61 mg, 21%), which were pure according to $^{31}\text{P}\{^1\text{H}\}$ NMR spectroscopy. After three days, significant decomposition of the compound dissolved in THF into **1** and further unidentified products was detected in the $^{31}\text{P}\{^1\text{H}\}$ NMR spectrum. In addition, also isolated crystals seem to decompose in a matter of hours. Therefore, characterization by IR spectroscopy and elemental analysis was not feasible. $^1\text{H}\{^{31}\text{P}\}$ NMR (THF- d_8): $\delta = 7.34$ (br, s, 15H, Ph), 1.30 (s, 18H, $(\text{H}_3\text{C})_3\text{C}-\text{P}_A$), 1.25 (s, 18H, $(\text{H}_3\text{C})_3\text{C}-\text{P}_B$), 1.05 (s, 18H, $(\text{H}_3\text{C})_3\text{C}-\text{P}_C$) ppm. $^{13}\text{C}\{^1\text{H}, ^{31}\text{P}\}$ NMR (THF- d_8): $\delta = 133.2$ (s, $\text{C}_{\text{arom.}}$), 128.1 (s, $\text{C}_{\text{arom.}}$), 127.9 (s, $\text{C}_{\text{arom.}}$), 127.5 (s, $\text{C}_{\text{arom.}}$), 33.6 (s, $\text{C}-\text{P}_A$), 29.9 (s, $\text{C}-\text{P}_B$), 29.7 (s, $\text{C}-\text{P}_C$), 29.1 (s, $(\text{H}_3\text{C})_3\text{C}-\text{CP}_A$), 28.8 (s, $(\text{H}_3\text{C})_3\text{C}-\text{CP}_B$), 27.7 (s, $(\text{H}_3\text{C})_3\text{C}-\text{CP}_C$) ppm. $^{31}\text{P}\{^1\text{H}\}$ NMR (THF- d_8): $\delta = 48.6$ (m, 2P, P_A), 23.9 (m, 1P, P_E), -26.9 (m, 2P, P_B), -44.6 (m, 2P, P_C), -58.2 (m, 2P, P_D) ppm. MS (ESI(+), MeCN): $m/z = 663.1$ $[\text{Pd}(\text{OPPh}_3)_2\text{H}]^+$ (54%), 721.1 $[\text{LPdO}_2\text{H}]^+$ (6%), 751.1 $[\text{LPdO}_2\text{Na}]^+$ (13%), 925.2 $[\text{Pd}(\text{OPPh}_3)_2(\text{PPh}_3)\text{H}]^+$ (22%). L = $\text{C}_{24}\text{H}_{54}\text{P}_8$.

Synthesis of [CuBr(1- κ^2P^2, P^4)] (6). A suspension of [CuBr(SMe₂)] (51 mg, 0.248 mmol, 1.0 eq) in 45 mL THF was added slowly to a solution of octaphosphine **1** (146 mg, 0.247 mmol, 1.0 eq) in 30 mL THF. The reaction mixture was stirred for one hour. Approximately 50 mL of solvent were removed under reduced pressure. Large yellow crystals were obtained by very slowly passing a stream of nitrogen over a solution of the sample in THF (161 mg, 89%). The compound showed no luminescent behavior. ¹H{³¹P} NMR (THF-*d*₈): δ = 1.39 (br, 18H, (H₃C)₃C-P_A), 1.30 (s, 18H, (H₃C)₃C-P_C), 1.15 (br, 18H, (H₃C)₃C-P_B) ppm. ¹³C{¹H, ³¹P} NMR (THF-*d*₈): δ = 32.8 (s, C-P_A), 32.7 (s, C-P_B), 31.9 (s, C-P_C), 29.9 (s, (H₃C)₃C-CP_A), 28.6 (s, (H₃C)₃C-CP_B), 27.9 (s, (H₃C)₃C-CP_C) ppm. ³¹P{¹H} NMR (THF-*d*₈): δ = -13.9 (m, 2P, P_A), -28.1 (m, 2P, P_B), -41.4 (m, 2P, P_C), -76.4 (m, 2P, P_D) ppm. IR (KBr): $\tilde{\nu}$ = 3351 (w), 2946 (s, $\nu_{\text{as}}(\text{C-H})$), 2889 (s, $\nu_{\text{s}}(\text{C-H})$), 2855 (s, $\nu_{\text{s}}(\text{C-H})$), 1467 (m), 1456 (s, $\delta_{\text{as}}(\text{CH}_3)$), 1389 (m, $\delta_{\text{s}}(\text{CH}_3)$), 1361 (s, $\delta_{\text{s}}(\text{CH}_3)$), 1241 (m), 1171 (s, $\rho(\text{CH}_3) + \nu_{\text{s}}(\text{C-C})$), 1009 (m, $\rho(\text{CH}_3)$), 984 (m), 938 (w, $\rho(\text{CH}_3) + \nu_{\text{s}}(\text{C-C})$), 805 (m, $\nu_{\text{s}}(\text{C-C})$), 745 (w), 652 (w), 573 (w), 506 (w), 467 (w), 414 (w) cm⁻¹. MS (ESI(+), MeCN): m/z = 653.1 [CuL]⁺ (100%), 669.1 [CuLO]⁺ (15%), 685.1 [CuLO₂]⁺ (24%), 797.0 [Cu₂BrL]⁺ (2%), 1387.2 [Cu₂BrL₂]⁺ (12%), 1403.2 [Cu₂BrL₂O₁]⁺ (1%). L = C₂₄H₅₄P₈. MP: 263 °C. EA (%) for C₂₄H₅₄CuBrP₈; calc. C 39.28, H 7.42; found C 38.90, H 7.30.

Synthesis of [{CuBr}₂(1- $\kappa^2P^2, P^2', \kappa^2P^4, P^4'$)] (7). A suspension of [CuBr(SMe₂)] (70 mg, 0.340 mmol, 2.0 eq) in 45 mL THF was added slowly to a solution of octaphosphine **1** (101 mg, 0.169 mmol, 1.0 eq) in 10 mL THF. The reaction mixture was stirred for one hour and filtered. Approximately 40 mL of solvent were removed under reduced pressure. Keeping the solution at 0 °C gave yellow crystals (127 mg, 72%). The compound showed no luminescent behavior. The dimerization of **7** could not be controlled in order to selectively obtain **8**, as oligomerization was

occurring simultaneously. A few single crystals of **8** were obtained from a test reaction in THF.

$^1\text{H}\{^{31}\text{P}\}$ NMR (THF- d_8): $\delta = 1.34$ (s, 18H, $(\text{H}_3\text{C})_3\text{C-P}_A$), 1.20 (s, 36H, $(\text{H}_3\text{C})-\text{P}_B$) ppm.

$^{13}\text{C}\{^1\text{H},^{31}\text{P}\}$ NMR (THF- d_8): $\delta = 34.1$ (s, C- P_B), 33.0 (s, C- P_A), 30.1 (s, $(\text{H}_3\text{C})_3\text{C-CP}_B$), 27.9 (s, $(\text{H}_3\text{C})_3\text{C-CP}_A$) ppm. $^{31}\text{P}\{^1\text{H}\}$ NMR (THF- d_8): $\delta = -17.0$ (m, 2P, P_A), -35.1 (m, 4P, P_B) -59.3 (m, 2P, P_C) ppm. IR (KBr): $\tilde{\nu} = 3192$ (w), 3085 (w), 3024 (w), 2951 (s, $\nu_{\text{as}}(\text{C-H})$), 2855 (s, $\nu_{\text{s}}(\text{C-H})$), 2742 (w), 2714 (w), 1603 (w), 1457 (s, $\delta_{\text{as}}(\text{CH}_3)$), 1392 (w, $\delta_{\text{s}}(\text{CH}_3)$), 1362 (s, $\delta_{\text{s}}(\text{CH}_3)$), 1170 (s, $\rho(\text{CH}_3 + \nu_{\text{s}}(\text{C-C}))$), 1081 (w), 1012 (m, $\rho(\text{CH}_3)$), 939 (w, $\rho(\text{CH}_3) + \nu_{\text{s}}(\text{C-C})$), 803 (m, $\nu_{\text{s}}(\text{C-C})$), 732 (m), 695 (w), 578 (w), 510 (w), 465 (w), 450 (w), 412 (w) cm^{-1} . MS (ESI(+), MeCN): $m/z = 653.1$ [CuL] $^+$ (92%), 669.1 [CuLO] $^+$ (28%), 685.1 [CuLO_2] $^+$ (5%), 701.1 [CuLO_3] $^+$ (3%), 796.1 [Cu_2BrL] $^+$ (98%), 812.1 [Cu_2BrLO] $^+$ (37%), 828.1 [Cu_2BrLO_2] $^+$ (4%), 940.8 [$\text{Cu}_3\text{Br}_2\text{L}$] $^+$ (29%), 1387.2 [Cu_2BrL_2] $^+$ (100%), 1403.2 [$\text{Cu}_2\text{BrL}_2\text{O}_1$] $^+$ (40%), 1419.2 [$\text{Cu}_2\text{BrL}_2\text{O}_2$] $^+$ (7%), 1433.2 [$\text{Cu}_2\text{BrL}_2\text{O}_3$] $^+$ (2%), 1531.0 [$\text{Cu}_3\text{Br}_2\text{L}_2$] $^+$ (55%), 1547.0 [$\text{Cu}_3\text{Br}_2\text{L}_2\text{O}$] $^+$ (2%), 1563.0 [$\text{Cu}_3\text{Br}_2\text{L}_2\text{O}_2$] $^+$ (2%), 1674.9 [$\text{Cu}_4\text{Br}_3\text{L}_2$] $^+$ (11%), 1674.9 [$\text{Cu}_4\text{Br}_3\text{L}_2\text{O}$] $^+$ (3%). L = $\text{C}_{24}\text{H}_{54}\text{P}_8$. MP: 270 °C. EA (%) for $\text{C}_{31}\text{H}_{62}\text{Cu}_2\text{Br}_2\text{P}_8$; calc. C 38.40, H 6.45; found C 37.79, H 6.40

Reaction of Octaphosphine 1 with *cis*-[PtCl₂(cod)] (formation of 9, 10 and 11). A suspension of octaphosphine **1** (126 mg, 0.213 mmol, 1.0 eq) in 6 mL toluene was added to *cis*-[PtCl₂(cod)] (93 mg, 0.248 mmol, 1.1 eq). The reaction mixture was heated under reflux for five days.

Evaporation of the solvent under reduced pressure gave an orange solid which was extracted with 7 mL Et₂O and with three times 7 mL THF. The phases were combined and filtered to give a clear deep red solution. This was kept at -30 °C to give light orange crystals (87 mg). For NMR assignments see Table 2.

ASSOCIATED CONTENT

Supporting Information.

Contains the NMR spectra of the compounds discussed above and additional information on the X-ray diffraction data (PDF).

Accession Codes.

CCDC 1979987 (**2**), CCDC 1979985 ([RhBr(CO)(1- κ^2 P²,P⁴)].0.5Et₂O), CCDC 1979986 ([RhBr(CO)(1- κ^2 P²,P⁴)].THF), CCDC 1979984 (**3**·C₇H₈), CCDC 1979988 (**4**), CCDC 1979989 (**4**·THF), CCDC 1979990 (**5**), CCDC 1979993 (**6**), CCDC 1979998 (**7**·0.0625THF), CCDC 1979991 (**7**·1.5C₆D₆), CCDC 1979994 (**7**·C₇H₈), CCDC 1979992 (**8**), CCDC 1979995 (**9**·THF), CCDC 1979996 (**10**·0.5Et₂O) and CCDC 1979997 (P₈^tBu₆O₆) contain the supplementary crystallographic data for this paper. These data can be obtained free of charge via <https://summary.ccdc.cam.ac.uk/structure-summary-form> (or from the Cambridge Crystallographic Data Centre, 12 Union Road, Cambridge CB2 1EZ, UK; fax: (+44)1223-336-033; or deposit@ccdc.cam.ac.uk).

AUTHOR INFORMATION

Corresponding Author

*E.H.: email, hey@uni-leipzig.de; tel. +49 341 97 36151

Funding Sources

This work was funded by the University of Leipzig (Germany).

ACKNOWLEDGMENT

We would foremost like to thank Dr. Sara Durini for the TG/DTA measurements. Furthermore, we thank Dr. Aslihan Kırçalı for crystallizing complex **2**, Prof. Dr. Juri Grin for analyzing the

PXRD pattern and Prof. Dr. Klaus Koch for his advice on the reaction kinetics of the complexes.
The Financial support from the Studienstiftung des deutschen Volkes (doctoral grant for T.G.)
and the Graduate School BuildMoNa are gratefully acknowledged.

ABBREVIATIONS

CIS, Coordination-induced shift; EA, Elemental analysis; MP, Melting point.

SYNOPSIS.



The octaphosphine **1** possesses eight possible donor atoms, promising a rich coordination chemistry. In fact, numerous complexes were obtained where the ligand adopts different conformations, coordinates metals with different donor atoms and also binds more than one metal atom, leading to six different coordination modes so far. Furthermore, these complexes can be converted to phosphorus-rich metal phosphides.

REFERENCES

References

- (1) Hoffmann, R. Building Bridges Between Inorganic and Organic Chemistry (Nobel Lecture). *Angew. Chem.* **1982**, *94*, 725–739. *Angew. Chem. Int. Ed.* **1982**, *21*, 711–724.
- (2) Köhler, H.; Michaelis, A. Ueber Phenylphosphin und Phosphobenzol (Diphosphenyl). *Ber. Dtsch. Chem. Ges.* **1877**, *10*, 807–814.
- (3) Boeck, G.; Peppel, T.; Selent, D.; Schulz, A. Der Phosphorchemiker August Michaelis in Rostock. *Nachr. Chem.* **2017**, *65*, 1030–1033.
- (4) Baudler, M.; Glinka, K. Contributions to the chemistry of phosphorus. 218. Monocyclic and polycyclic phosphines. *Chem. Rev.* **1993**, *93*, 1623–1667.
- (5) Baudler, M.; Glinka, K. Open-Chain Polyphosphorus Hydrides (Phosphines). *Chem. Rev.* **1994**, *94*, 1273–1297.
- (6) Yoshifuji, M.; Shima, I.; Inamoto, N.; Hirotsu, K.; Higuchi, T. Synthesis and structure of bis(2,4,6-tri-tert-butylphenyl)diphosphene: Isolation of a true phosphobenzene. *J. Am. Chem. Soc.* **1981**, *103*, 4587–4589.
- (7) Baudler, M.; Akpapgolou, S.; Ouzounis, D.; Wasgestian, F.; Meinigke, B.; Budzikiewicz, H.; Münster, H. On the Pentaphosphacyclopentadienide Ion, P₅(-). *Angew. Chem.*, **1988**, *2*, 288–289. *Angew. Chem. Int. Ed.* **1988**, *27*, 280–281.
- (8) Dillon, K. B.; Mathey, F.; Nixon, J. F. *Phosphorus: The carbon copy ; from organophosphorus to phospho-organic chemistry*; Wiley: Chichester, 1998.
- (9) Fritz, G.; Schneider, H.-W.; Höhle, W.; Schnering, H. G. von. Komplexchemie P-reicher Phosphane und Silylphosphane. I. Zur Komplexchemie der Heptaphospha-nortricyclane R₃P₇ (R = Et, i-Pr). *Z. Anorg. Allg. Chem.* **1990**, *584*, 21–50.
- (10) Wolf, R.; Schisler, A.; Lönnecke, P.; Jones, C.; Hey-Hawkins, E. Syntheses and Molecular Structures of Novel Alkali Metal Tetraorganylcyclopentaphosphanides and Tetraorganyltetraphosphane-1,4-diides. *Eur. J. Inorg. Chem.* **2004**, *2004*, 3277–3286.
- (11) Gómez-Ruiz, S.; Wolf, R.; Bauer, S.; Bittig, H.; Schisler, A.; Lönnecke, P.; Hey-Hawkins, E. Coordination chemistry of the cyclo-(P₅tBu₄)(-) ion: Monomeric and oligomeric copper(I), silver(I) and gold(I) complexes. *Chem. Eur. J.* **2008**, *14*, 4511–4520.
- (12) Gómez-Ruiz, S.; Hey-Hawkins, E. The versatile reactivity of tetra-tert-butyl-cyclopentaphosphanide monoanions. *New J. Chem.* **2010**, *34*, 1525–1532.
- (13) Gómez-Ruiz, S.; Hey-Hawkins, E. The unusual coordination chemistry of phosphorus-rich linear and cyclic oligophosphanide anions. *Coord. Chem. Rev.* **2011**, *255*, 1360–1386.

- (14) Adhikari, A. K.; Sárosi, M. B.; Grell, T.; Lönnecke, P.; Hey-Hawkins, E. Unusual Reactivity of Sodium Tetramesityltetraphosphanediide towards Cyclohexyl Isocyanide. *Chem. Eur. J.* **2016**, *22*, 15664–15668.
- (15) Adhikari, A. K.; Sárosi, M. B.; Grell, T.; Lönnecke, P.; Hey-Hawkins, E. 16-Gliedriger Au₈P₈ -Makrocyclus aus Gold(I) und Diphospha(III)-guanidin. *Angew. Chem. Int. Ed.*, **2017**, *56*, 4061–4064. *Angew. Chem.* **2017**, *129*, 4120–4123.
- (16) Kircali, A.; Lönnecke, P.; Hey-Hawkins, E. Synthesis and Thermolysis of the Homoleptic Iron(II) Complex [Fe{cyclo-(P^tBu₄)₂}₂]. *Z. Anorg. Allg. Chem.* **2014**, *640*, 271–274.
- (17) Kircali, A.; Frank, R.; Gómez-Ruiz, S.; Kirchner, B.; Hey-Hawkins, E. Synthesis and Thermolysis of the Phosphorus-Rich Manganese(I) Complex [Mn₂(μ-Br){cyclo-(P^tBu₃)PtBu}(CO)₆]: From Complexes to Metal Phosphides. *ChemPlusChem* **2012**, *77*, 341–344.
- (18) Yufanyi, D. M.; Grell, T.; Sárosi, M.-B.; Lönnecke, P.; Hey-Hawkins, E. Group 6 metal carbonyl complexes of cyclo-(P⁵Ph₅). *Pure Appl. Chem.* **2019**, *91*, 785–796.
- (19) Schnering, H. G. von; Hoenle, W. Chemistry and structural chemistry of phosphides and polyphosphides. 48. Bridging chasms with polyphosphides. *Chem. Rev.* **1988**, *88*, 243–273.
- (20) Grell, T.; Hey-Hawkins, E. Dynamic Gold (I) Complexes of Hexa-tert-butyl-octaphosphane. *Eur. J. Inorg. Chem.* **2020**, *2020*, 732–736.
- (21) Grell, T.; Hey-Hawkins, E. Unexpected Isomerization of Hexa-tert-butyl-octaphosphane. *Chem. Eur. J.* **2019**, *26*, 1008–1012.
- (22) A. Kircali. Dissertation, Leipzig University, 2012.
- (23) Okuniewski, A.; Rosiak, D.; Chojnacki, J.; Becker, B. Coordination polymers and molecular structures among complexes of mercury(II) halides with selected 1-benzoylthioureas. *Polyhedron* **2015**, *90*, 47–57.
- (24) Coe, B. J.; Glenwright, S. J. Trans-effects in octahedral transition metal complexes. *Coord. Chem. Rev.* **2000**, *203*, 5–80.
- (25) Riegel, B.; Pfitzner, A.; Heckmann, Y. G.; Binder, H.; Fluck, E. In situ-Erzeugung von [PX] und Insertion in (tBuP)₃, (X = Cl, Br) Synthese der funktionalisierten Cyclophosphane (tBuP)₃PX, [(tBu)(X)P-2,3,4-(tBu)₃]P₄ und Strukturbestimmung von (tBuP)₃PCl. *Z. Anorg. Allg. Chem.* **1995**, *621*, 1365–1372.
- (26) Baudler, M.; Tschäbunin, H. Beiträge zur Chemie des Phosphors. 138. P₅(t-Bu)₄H - das erste Derivat von iso-P₅H₅. *Z. Anorg. Allg. Chem.* **1984**, *511*, 77–83.
- (27) Schmidt, R.; Moya, S. A.; Villagra, D.; Binder, H.; Heckmann, Y. G. Reaccion de bromuro de oro(III) con tetra-fer-butyl-ciclotetrafosfina. *J. Chil. Chem. Soc.* **1996**, *41*, 371–375.
- (28) Fritz, G.; Härer, J.; Stoll, K. Untersuchungen zur Metallierung der Cyclophosphane P₄(Cme₃)₃(Sime₃), P₄(Cme₃)₂(Sime₃)₂, P₄(Sime₃)₄. *Z. Anorg. Allg. Chem.* **1983**, *504*, 47–54.

- (29) Baudler, M.; Aktalay, Y.; Tebbe, K.-F.; Heinlein, T. tBu₄P₆, ein neues bicyclisches Organophosphan. *Angew. Chem. Int. Ed. Engl.*, **1981**, *20*, 967–969. *Angew. Chem.* **1981**, *93*, 1020–1022.
- (30) Baudler, M.; Michels, M.; Hahn, J.; Pieroth, M. P₇tBu₅ - das erste Bicyclo[3.2.0]heptaphosphan. *Angew. Chem. Int. Ed. Engl.*, **1985**, *24*, 504–505. *Angew. Chem.* **1985**, *97*, 514–515.
- (31) Burck, S.; Götz, K.; Kaupp, M.; Nieger, M.; Weber, J.; Schmedt auf der Günne, J.; Gudat, D. Diphosphines with strongly polarized P-P bonds: Hybrids between covalent molecules and donor-acceptor adducts with flexible molecular structures. *J. Am. Chem. Soc.* **2009**, *131*, 10763–10774.
- (32) Dyer, G.; Wharf, R. M.; Hill, W. E. ³¹P NMR studies of cis-[RhCl(CO)(bis-phosphine)] complexes. *Inorg. Chim. Acta* **1987**, *133*, 137–140.
- (33) Gonsalvi, L.; Adams, H.; Sunley, G. J.; Ditzel, E.; Haynes, A. Steric and Electronic Effects on the Reactivity of Rh and Ir Complexes Containing P–S, P–P, and P–O Ligands. Implications for the Effects of Chelate Ligands in Catalysis. *J. Am. Chem. Soc.* **2002**, *124*, 13597–13612.
- (34) Hahn, J. Higher Order ³¹P NMR Spectra of Polyphosphorus Compounds. In *Phosphorus-31 NMR spectroscopy in stereochemical analysis*; Verkade, J. G., Ed.; Methods in stereochemical analysis 8; VCH: Weinheim, 1987.
- (35) Berger, S.; Braun, S.; Kalinowski, H.-O. ³¹P-NMR-Spektroskopie; NMR-Spektroskopie von Nichtmetallen / Stefan Berger; Siegmund Braun; Hans-Otto Kalinowski ; Bd. 3; Thieme: Stuttgart, 1993.
- (36) Baudler, M.; Germeshausen, J. P₈tBu₆O₆ – ein hochoxidiertes Cyclophosphan mit intaktem P-Gerüst. *Angew. Chem. Int. Ed. Engl.*, **1987**, *26*, 348–349. *Angew. Chem.* **1987**, *99*, 372–373.
- (37) Ellermann, J.; Köck, E.; Zimmermann, H.; Gomm, M. Chemie polyfunktioneller molekule. *J. Organomet. Chem.* **1988**, *345*, 167–176.
- (38) Brunner, H.; Faustmann, P.; Nuber, B. Optically active transition metal compounds 113. *J. Organomet. Chem.* **1998**, *556*, 129–140.
- (39) Saito, T.; Sawada, S. ⁵⁹Co Quadrupole Effects on the ¹H, ³¹P, and ⁵⁹Co NMR Spectra of HFeCo₃(CO)₉ [P(OCH₃)₃]₃ and the ¹H NMR Spectra of Other Derivatives. *Bull. Chem. Soc. J.* **1985**, *58*, 459–463.
- (40) Lin, J. T.; Wang, S. Y.; Chou, Y. C.; Gong, M. L.; Shioh, Y.-M. Diphenylphosphine derivatives of Co(NO)(CO)₃, Fe(NO)₂(CO)₂ and Mn(NO)(CO)₄. *J. Organomet. Chem.* **1996**, *508*, 183–193.
- (41) Hieber, W.; Ellermann, J. Substitutionsreaktionen des Kobaltnitrosylcarbonyls. *Chem. Ber.* **1963**, *96*, 1643–1649.

- (42) Mawby, R. J.; Morris, D.; Thorsteinson, E. M.; Basolo, F. Chelate and Bridge Complexes of Metal Carbonyl Compounds with a Ditertiary Phosphine: A Study of Their Formation and Interconversion. *Inorg. Chem.* **1966**, *5*, 27–33.
- (43) Brunner, H.; Faustmann, P.; Dietl, A.; Nuber, B. Optically active transition metal compounds 112. Synthesis of chiral carbonylnitrosylcobalt complexes with bidentate PP*, PN* and NN* ligands. *J. Organomet. Chem.* **1997**, *542*, 255–263.
- (44) Albano, V. G.; Bellon, P. L.; Ciani, G. Stereochemistry of tetrahedral complexes of group VIII metals. *J. Organomet. Chem.* **1972**, *38*, 155–165.
- (45) Grushin, V. V.; Marshall, W. J. Facile Ar-CF₃ bond formation at Pd. Strikingly different outcomes of reductive elimination from (Ph₃P)₂Pd(CF₃)Ph and (Xantphos)Pd(CF₃)Ph. *J. Am. Chem. Soc.* **2006**, *128*, 12644–12645.
- (46) Tsubomura, T.; Ito, Y.; Inoue, S.; Tanaka, Y.; Matsumoto, K.; Tsukuda, T. Strongly luminescent palladium(0) and platinum(0) diphosphine complexes. *Inorg. Chem.* **2008**, *47*, 481–486.
- (47) Bolm, C.; Kaufmann, D.; Gessler, S.; Harms, K. Crystal structure of a new chiral Pd(0) / diphosphine complex and its use in enantioselective allylic alkylations. *J. Organomet. Chem.* **1995**, *502*, 47–52.
- (48) Tsuge, K. Luminescent Complexes Containing Halogeno-bridged Dicopper(I) Unit {Cu₂(μ-X)₂} (X = Cl, Br, and I). *Chem. Lett.* **2013**, *42*, 204–208.
- (49) Verkade, J. G.; Mosbo, J. A. Stereospecificity in ³¹P-Element Couplings: One-Bond Couplings to other Nonmetals and to Metals. In *Phosphorus-31 NMR spectroscopy in stereochemical analysis*; Verkade, J. G., Ed.; Methods in stereochemical analysis 8; VCH: Weinheim, 1987.
- (50) Fritz, G.; Schneider, H.-W.; Höhle, W.; Schnering, H. G. von. Komplexchemie P-reicher Phosphane und Silylphosphane. III. Die Komplexverbindungen (t-Bu)₃P₉ Cr(CO)₅ und (t-Bu)₃P₉ 2 Cr(CO)₅ des Nonaphosphans(3), (t-Bu)₃P₉. *Z. Anorg. Allg. Chem.* **1990**, *585*, 51–64.
- (51) Hynes, M. J.; Brannick, P. F. The Rates and Mechanisms of Substitution of Square-Planar Complexes of Ni (II), Pd(II), AND Pt(II) Containing Bidentate Sulphur Ligands in Water and Methanol. *Proc. Royal Ir. Acad. B* **1977**, 479–493.
- (52) Kjekshus, A.; Nølander, B.; Klæboe, P.; Cyvin, S. J.; Lagerlund, I.; Ehrenberg, L. On the Properties of Binary Compounds with the CoSb₂ Type Crystal Structure. *Acta Chem. Scand.* **1971**, *25*, 411–422.
- (53) J. A. McCleverty; G. Wilkinson. Dichlorotetracarbonylrhodium. *Inorg. Synth.* **1966**, 211–214.
- (54) Park, I.-H.; So, M.-S.; Park, K.-H. Facile Preparation of Copper(I) Halide-Dimethyl Sulfide Complex and Its Application. *Bull. Kor. Chem. Soc.* **2007**, *28*, 1515–1518.

- (55) Harris, R. K.; Becker, E. D.; Cabral De Menezes, S. M.; Goodfellow, R. J.; Granger, P. NMR nomenclature: Nuclear spin properties and conventions for chemical shifts (IUPAC recommendations 2001). *Concepts Magn. Reson.* **2002**, *14*, 326–346.
- (56) Albrand, J. P.; Cogne, A.; Robert, J. B. Cyclotetraphosphanes: Geometry, 1J(PP) nuclear magnetic resonance coupling constants, and phosphorus chemical shift anisotropy. A nuclear magnetic resonance study in liquid crystals. *J. Am. Chem. Soc.* **1978**, *100*, 2600–2604.
- (57) Agilent Technologies Ltd. *CrysAlis-Pro Software package*, 2014.
- (58) Altomare, A.; Cascarano, G.; Giacovazzo, C.; Guagliardi, A.; Burla, M. C.; Polidori, G.; Camalli, M. SIRPOW.92 – a program for automatic solution of crystal structures by direct methods optimized for powder data. *J. Appl. Crystallogr.* **1994**, *27*, 435–436.
- (59) Sheldrick, G. M. SHELXT - integrated space-group and crystal-structure determination. *Acta Cryst. A* **2015**, *71*, 3–8.
- (60) Farrugia, L. J. WinGX and ORTEP for Windows: An update. *J. Appl. Crystallogr.* **2012**, *45*, 849–854.
- (61) STOE Cie GmbH. *WinXPow*, 2014.
- (62) Bruker. *Topas*, 2014.
- (63) Neese, F. The ORCA program system. *WIREs Comput. Mol. Sci.* **2012**, *2*, 73–78.
- (64) Grimme, S.; Antony, J.; Ehrlich, S.; Krieg, H. A consistent and accurate ab initio parametrization of density functional dispersion correction (DFT-D) for the 94 elements H-Pu. *J. Chem. Phys.* **2010**, *132*, 154104.
- (65) Grimme, S.; Ehrlich, S.; Goerigk, L. Effect of the damping function in dispersion corrected density functional theory. *J. Comput. Chem.* **2011**, *32*, 1456–1465.
- (66) Sinnecker, S.; Rajendran, A.; Klamt, A.; Diedenhofen, M.; Neese, F. Calculation of solvent shifts on electronic g-tensors with the conductor-like screening model (COSMO) and its self-consistent generalization to real solvents (direct COSMO-RS). *J. Phys. Chem. A* **2006**, *110*, 2235–2245.
- (67) Schwerdtfeger, P.; Dolg, M.; Schwarz, W. H. E.; Bowmaker, G. A.; Boyd, P. D. W. Relativistic effects in gold chemistry. I. Diatomic gold compounds. *J. Chem. Phys.* **1989**, *91*, 1762–1774.
- (68) Weigend, F.; Ahlrichs, R. Balanced basis sets of split valence, triple zeta valence and quadruple zeta valence quality for H to Rn: Design and assessment of accuracy. *Phys. Chem. Chem. Phys.* **2005**, *7*, 3297–3305.
- (69) Zhao, Y.; Truhlar, D. G. A new local density functional for main-group thermochemistry, transition metal bonding, thermochemical kinetics, and noncovalent interactions. *J. Chem. Phys.* **2006**, *125*, 194101.

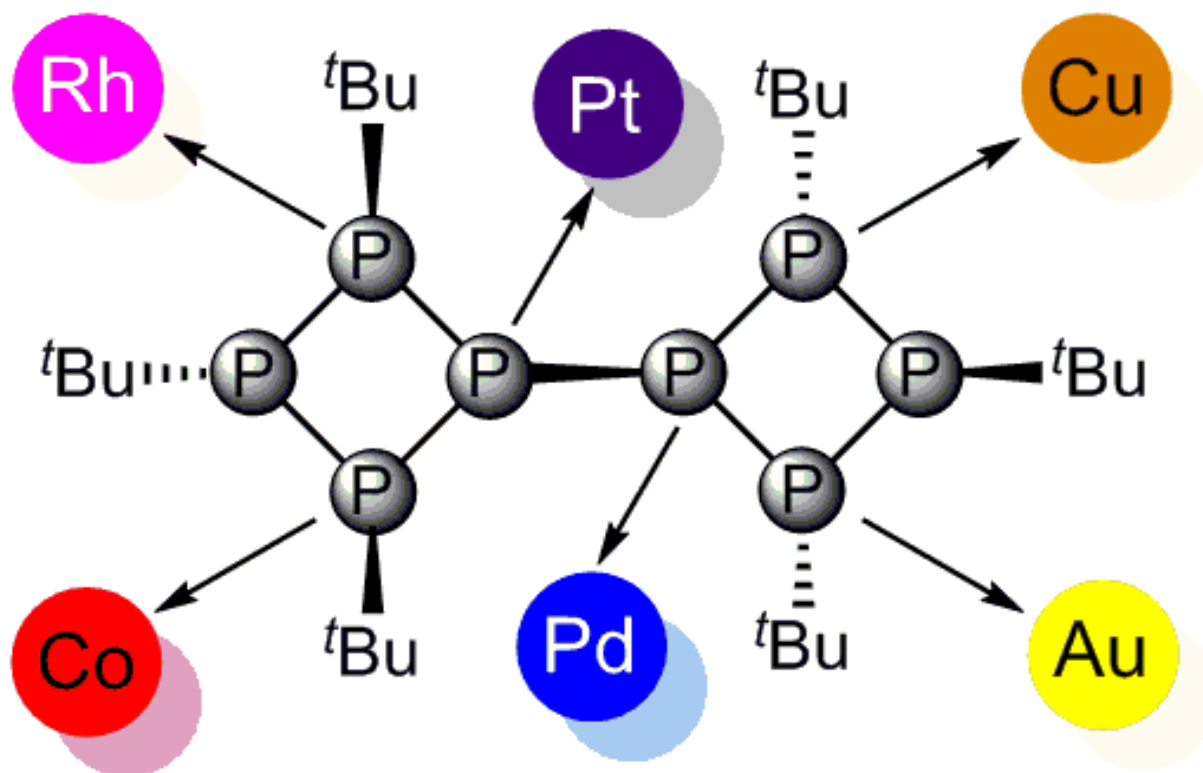
(70) Schäfer, A.; Horn, H.; Ahlrichs, R. Fully optimized contracted Gaussian basis sets for atoms Li to Kr. *J. Chem. Phys.* **1992**, *97*, 2571–2577.

(71) Schäfer, A.; Huber, C.; Ahlrichs, R. Fully optimized contracted Gaussian basis sets of triple zeta valence quality for atoms Li to Kr. *J. Chem. Phys.* **1994**, *100*, 5829–5835.

(72) Kim, K.; Jordan, K. D. Comparison of Density Functional and MP2 Calculations on the Water Monomer and Dimer. *J. Phys. Chem.* **1994**, *98*, 10089–10094.

(73) Stephens, P. J.; Devlin, F. J.; Chabalowski, C. F.; Frisch, M. J. Ab Initio Calculation of Vibrational Absorption and Circular Dichroism Spectra Using Density Functional Force Fields. *J. Phys. Chem.* **1994**, *98*, 11623–11627.

SYNOPSIS.



The octaphosphine 1 possesses eight possible donor atoms, promising a rich coordination chemistry. In fact, numerous complexes were obtained where the ligand adopts different conformations, coordinates metals with different donor atoms and also binds more than one

metal atom, leading to six different coordination modes so far. Furthermore, these complexes can be converted to phosphorus-rich metal phosphides.